Available online at www.sciencedirect.com

SCIENCE DIRECT

Developmental Biology 279 (2005) 462–480

DEVELOPMENTAL BIOLOGY

www.elsevier.com/locate/ydbio

Genomes & Developmental Control

Candidate downstream regulated genes of HOX group 13 transcription factors with and without monomeric DNA binding capability

Thomas M. Williams[a], Melissa E. Williams[a], Rork Kuick[b], David Misek[b], Kevin McDonagh[c], Samir Hanash[b], Jeffrey W. Innis[a,b,*]

[a]*Department of Human Genetics, University of Michigan, Ann Arbor, MI 48109-0618, USA*
[b]*Department of Pediatrics, University of Michigan, Ann Arbor, MI 48109-0618, USA*
[c]*Department of Internal Medicine, University of Michigan, Ann Arbor, MI 48109-0618, USA*

Received for publication 27 August 2004, revised 24 November 2004, accepted 6 December 2004

Abstract

Hox genes encode transcription factors that regulate the morphogenesis of developing embryos. In mammals, knowledge of the genetic pathways, including the possible direct or indirect targets, regulated by HOX proteins is extremely limited. To identify the downstream genes regulated by posterior HOX proteins, we expressed HOXA13 in mouse embryonic fibroblasts lacking paralog group 13 expression using a bicistronic HOXA13/EGFP retroviral vector. Microarray analysis identified 68 genes with significant, reproducible RNA expression changes (50 activated; 18 repressed) in stable HOXA13-expressing cells. Genes with the GO annotation terms "extracellular matrix" and "basement membrane" were greatly overrepresented, and several were shown to be regulated by HOX proteins in other studies. Among the genes strongly activated by HOXA13 were *Enpp2*, a bifunctional enzyme known to modulate tumor and normal cell motility and which is expressed in precartilaginous condensations; *Fhl1*, a transcription factor implicated in muscle cell differentiation and development; and *M32486*, a putative integral membrane molecule expressed in the female reproductive tract. Expression differences in the HOXA13-expressing cells were confirmed for selected downstream genes using semi-quantitative RT-PCR, and in vivo coexpression with *Hoxa13* in the limb interdigital mesenchyme was demonstrated for many. For two candidates, *Igfbp4* and *Fstl*, interdigital limb bud expression was reduced in *Hoxa13* mutants. To explore whether paralogous and nonparalogous HOX proteins could regulate the same genes, we created new HOX cell lines and examined the expression of selected genes identified by the HOXA13 screen. HOXD13 similarly activated/repressed 6 tested candidates, demonstrating that multiple downstream genetic pathways may be regulated by paralog HOX proteins. In contrast, HOXA9 was only able to repress expression of some gene targets. A HOXD13 mutant, HOXD13$^{IQN > AAA}$, incapable of monomeric DNA-binding, activated the expression of 5 HOXA13-upregulated genes; but was incapable of repressing the expression of *Ngef* and *Casp8ap2*. Our results suggest that HOX protein–protein interactions without direct HOX DNA-binding may play a larger role in HOX transcriptional regulation than generally assumed, and DNA-binding appears critical for repression.

Keywords: HOXA13; Hox; Homeodomain; Transcription factor; Limb bud; Target genes; Realizators

Introduction

Hox genes encode a family of evolutionarily conserved transcription factors that play a fundamental role in patterning the anteroposterior axis of developing embryos (Krumlauf, 1994; McGinnis and Krumlauf, 1992). Each protein contains a 60 amino acid DNA-binding domain known as the homeodomain (HD) (Gehring et al., 1994a). There are 39 mammalian *Hox* genes that are arranged in 4 linkage groups (A–D), each on a different chromosome. *Hox* genes have been numbered 1–13 based on their positions within each cluster; however, no single cluster has the full complement of 13 genes due to gene loss. Genes

* Corresponding author. Department of Human Genetics, University of Michigan, Med. Sci. II 4811, Ann Arbor, MI 48109-0618, USA.
Fax: +1 734 763 3784.
E-mail address: innis@umich.edu (J.W. Innis).

0012-1606/$ - see front matter © 2004 Elsevier Inc. All rights reserved.
doi:10.1016/j.ydbio.2004.12.015

at equivalent positions in each of the clusters are referred to as paralogs since their HDs are more similar to other paralog members than those adjacent to them within the cluster (McGinnis and Krumlauf, 1992; Ruddle et al., 1994). Loss-of-function studies have demonstrated redundant functions for paralogous as well as non-paralogous *Hox* genes (Favier et al., 1996; Kondo et al., 1998; Zakany and Duboule, 1996). Whereas differences in paralog group function are well delineated in the literature (Goff and Tabin, 1997; Zhao and Potter, 2001, 2002), phenotypic variations in individual *Hox* gene null phenotypes seem likely to be related to quantitative differences between paralog gene expression within individual cells (Greer et al., 2000; Wellik and Capecchi, 2003). Despite the well-described redundant functions, at least in terms of gross phenotype, individual differences in paralogous protein sequence and tissue expression suggests that at some level, unique functions are likely to exist for individual members of a paralogous group. Such qualitative characteristics acquired by divergent duplicated genes are underemphasized.

All HOX HDs contain identical DNA-base contacting residues consistent with their documented ability to bind similar DNA sequences (Laughon, 1991), yet cofactors can affect the affinity and specificity by which HOX proteins bind DNA (LaRonde-LeBlanc and Wolberger, 2003; Mann and Affolter, 1998). The similarity in DNA site recognition and the minimal differences in affinity for sites between individual proteins has created a conundrum of how specificity is achieved, and two basic models have been proposed to reconcile these observations: co-selective binding and widespread binding (Biggin and McGinnis, 1997). In the first, cofactors, which bind DNA cooperatively with the HOX protein, direct HOX proteins to specific targets. In the second model, HOX proteins are bound at many different sites in the genome, and cofactors may alter the activity of HOX proteins in transcriptional regulation of specific genes. Both models have support, although work in *Drosophila* has demonstrated that homeodomain proteins occupy a vast number of sites in vivo and are involved in the regulation of greater than 25% of expressed genes (Liang and Biggin, 1998; Walter et al., 1994).

If widespread binding also occurs in vertebrates, then work to identify mammalian HOX-regulated targets would enhance our understanding of the role of HOX protein abundance in regulatory mechanisms as well as differences between paralog groups in phenomena such as posterior prevalence. Under the widespread binding model HOX proteins would regulate a large set of common targets. Thus, theoretically, virtually any cell type would be suitable to identify HOX downstream genes and DNA-binding targets. Despite the apparent simplicity of this argument, our knowledge of HOX-regulated genes in mammals is very limited (Boudreau and Varner, 2004; Bromleigh and Freedman, 2000; Bruhl et al., 2004; Chen and Ruley, 1998; Dorsam et al., 2004; Edelman and Jones, 1995; Goomer et al., 1994; Jones et al., 1992, 1993; Stadler et al., 2001; Valerius et al., 2002), and cis-acting sequences on which these proteins exert their effects are few (Bruhl et al., 2004; Chen and Ruley, 1998; Ferretti et al., 2000; Jacobs et al., 1999). Moreover, the identification of targets in *Hox* mutant animals is complicated by the fact that coexpressed paralogous and non-paralogous HOX proteins provide redundant functions. This paucity of known regulated genes and authentic cis-acting sequences makes it difficult to understand the details of HOX protein function. Such aspects that need to be addressed include HOX protein domain requirements, cofactors, necessity for direct HOX DNA-binding, sites of interaction on chromatin, and the extent of regulation by paralogous and non-paralogous HOX proteins.

In this paper, we describe reproducible, endogenous gene expression changes associated with the expression of a HOX transcription factor. In this study, we do not differentiate between direct or indirect downstream targets. We exploited (1) an experimental context devoid of expression from other paralog group 13 genes to study the effect of HOXA13 at the transcriptional level using microarrays, and (2) the dominance of posterior gene products in function over anterior orthologs (Duboule and Morata, 1994; Goff and Tabin, 1997; Zhao and Potter, 2001).

Materials and methods

Retroviral vectors and cell lines

IRES-EGFP was subcloned from pIRES2-EGFP (Clontech) into the pGEM5ZF plasmid (Promega), which had been modified to contain an *Eco*RI site. *Hoxa13* cDNA was subcloned from pCMV+ (Post et al., 2000) into the *Eco*RI site 5′ of the IRES-EGFP element. An *Age*I/*Xho*I *Hoxa13*-IRES-EGFP and IRES-EGFP-only fragment was then cloned into the *Age*I/*Xho*I sites of pRET2, a MoMLV-based retroviral vector (Yang et al., 2002) at the respective sites. *Hoxd13*, HOXD13$^{IQN > AAA}$, and *Hoxa9* cDNAs were amplified by PCR and subcloned into the *Age*I/*Eco*RI sites 5′ of the IRES element.

All cell work was done using high glucose DMEM media (GIBCO-BRL) supplemented with 10% FBS, 100 U/ml penicillin, 100 μg/ml streptomycin, and 2 mM L-glutamine (GIBCO-BRL). Phoenix-A amphotropic packaging cells, from Gary Nolan (Stanford University, USA), were transfected with retroviral vectors using the calcium phosphate Pro-Fection kit (Promega). Retrovirus containing supernatants were collected at 24, 48, and 72 h post-transfection from amphotropic cells, filtered through a .45 μM filter (Nalgene) and each collection was separately incubated for 24 h with GP + E86 (derived from mouse 3T3 cells) ecotropic packaging cells (Markowitz et al., 1990). After 72 h, homogeneous populations of infected GP + E86 cells were isolated by GFP-based FACS. These cell lines were than expanded and used for stable

transgene expression and ecotropic virus production. NIH 3T3 and C3H 10T1/2 cells were transinfected with filtered supernatants from HOXA13/EGFP and EGFP-only ecotropic producer cells for 24 h. Enriched populations of infected cells expressing the transgenes were collected 48 h post-infection.

Immunocytochemistry

NIH 3T3 cells were plated on cover slips 24 h prior to transinfection with either HOXA13/EGFP or EGFP-only viral supernatants. 48 h post-transinfection, HOXA13 expression was analyzed as previously described (Post et al., 2000) with the following changes: fixation of cells was done using 4% formaldehyde; rabbit anti-HOXA13 primary antibody (Post et al., 2000) at a dilution of 1:200; goat anti-rabbit rhodamine-conjugated secondary antibody (Santa Cruz Biotechnology) at 1:500; cover slips mounted on slides with VECTASHIELD mounting media containing DAPI (Vector Labs). Photography was done using a Zeiss Axioplan fluorescent microscope.

RNA isolation, cRNA synthesis, and gene expression profiling

RNA was prepared from stable cell lines and transinfected cells. HOXA13/EGFP and EGFP-only GP + E86 stable viral producers (3 separate preparations), as well as FACS enriched (EGFP-based) NIH 3T3 and 10T1/2 cells 48 h post-transinfection with ecotropic HOXA13/EGFP or EGFP-only retroviruses (2 separate preparations) were homogenized in the presence of Trizol reagent (Invitrogen) and total cellular RNA was purified according to the manufacturer's procedures. This study utilized commercially available high-density microarrays that produce gene expression levels on 12,488 known mouse genes and expressed sequence tags (Affymetrix; MG_U74Av2). The preparation of cRNA, hybridization, and scanning of the arrays were performed according to the manufacturer's protocols, as previously reported (Beer et al., 2002; Schwartz et al., 2002). Probe intensities were extracted from the images using Affymetrix software (Microarray Suite 5.0).

Each probe set on the MG_U74Av2 arrays is composed of numerous (~16) 25-base oligonucleotides complementary to a specific cRNA called perfect match (PM) probes, and ~16 mismatch probes (MM) with sequences identical to the PM's except for alteration at the central base. Publicly available software was used to process the probe intensities (http://dot.ped.med.umich.edu:2000/pub/hox/index.html), using a GFP-only transinfected 3T3 array as the standard. Probe pairs for which PM − MM < −100 on the standard were removed from the analysis. Then, for each probe set on each array, PM−MM differences were trimmed by discarding the 25% highest and lowest differences, and the remaining differences averaged. The resulting raw intensities for each array were normalized to the standard using a piece-wise linear function that made 99 evenly spaced quantiles agree with the corresponding quantiles in the distribution of the standard. Fold changes were computed as the ratio of group means, after first replacing means that were <100 by 100. Normalized intensities were log-transformed in Excel spreadsheet (Microsoft) by mapping x to $\log(\max(x + 100,0) + 100)$. Linear models (ANOVAs) were fit to the log-transformed data that contained effects for the stable expressing and transinfected cells, the treatment differences (HOXA13/EGFP vs. EGFP-only), treatment by cell line interactions, and effects for the replicate experiments for each cell line. P values from resulting F statistics were calculated. The inclusion of microarray data from the transinfected cells aided the statistical comparison for the stable expressing cells by improving the calculation of variance. Enriched Gene Ontology terms were identified as previously described (Creighton et al., 2003). More information is available at the aforementioned web site.

Transient transfections and Western blotting

The stable expressing EGFP-only cells were transfected with pCMV-cDNA expression vectors for *Hoxa13* (Post and Innis, 1999b) and *Hoxd13*. In brief, 24 h prior to transfection, 400,000 cells were seeded in 6 cm dishes (4 per condition). Transfections were performed using the Fugene 6 reagent (Roche) following the manufacturer's protocol. 55 h post transfection, for each condition, RNA was prepared from 3 dishes using the Trizol protocol (Invitrogen). The fourth dish for each condition was used for protein preparation. Cells were treated with trypsin, pelleted by centrifugation and solubilized in 60 mM Tris, pH 6.8, 2% SDS, 10 mM EDTA, 10 mM EGTA, and 10% glycerol. Protein lysates were separated by electrophoresis using 12% SDS-polyacrylamide gel, and proteins were subsequently transferred to nitrocellulose. Western analysis used primary antibodies at 1:10,000 for rabbit anti-HOXA13 (Post et al., 2000), anti-HOXD13 (MAP-peptide with HOXD13 amino acids 176–198), 1:1000 for anti-HOXA9 (Upstate Biotechnology), and 1:15,000 for donkey anti-rabbit HRP-conjugated secondary antibody (Amersham), each in PBST with 5% Carnation nonfat dry milk. Protein expression was visualized using Supersignal chemilluminescent substrate (Pierce).

RT-PCR

All RT-PCR experiments were performed using the One-Step RT-PCR kit (Invitrogen) where the RT step was for 30 min at 50°C; the PCR used an annealing temperature of 56°C and an extension time of 45 s at 72°C for 40 cycles. Each primer pair was designed to amplify products spanning multiple exons, thus distinguishing spliced mRNA from genomic DNA amplification. Semi-quantitative RT-PCR,

for verifying general expression differences identified by microarray experiments, was performed using serial dilutions of total cellular RNA at final concentrations of 10,000, 2500, 625, 156, and 39 pg/μl. Control reactions were done separately using 100 ng of murine genomic DNA or water replacing the volume of input RNA. In vivo gene expression was analyzed by RT-PCR using 300 ng of total RNA isolated from mouse E12.5 forelimb autopods and 10-week-old female cervix/vagina segments. The RT-PCR primer pairs are: *Anxa8* (CAGGATGGCCTGGTGGAAAGC) and (CCTGGATCCACAAAGCCGCTC), *Blnk* (AGGCCCTCCAAGTGTTCCTCG and ACAGTCCCTGGAGGCGACATG), *Casp8ap2* (ACCATGGCAGCAGATGATGAC) and (CCAAATGGGGAGATGTGGACTG), *Col3a1* (CACAGTTCTAGAGGATGGCTG) and (GCCCTTCCAGATACTTGCAAG), *Enpp2* (TGCTCAGAAGACTGCTTGTCC and CAGGCTGCTCGGAGTAGAAGG), *Fabp4* (CTGGAAGACAGCTCCTCCTCG and GCCTCTTCCTTTGGCTCATGC), *Fbn1* (ATGAATGTCAGGCCATCCCAG and GGGTTCTTCTCACACTCATCC), *Fhl1* (ATAAGGTGGGCACCATGTCGG and GTGATTCCTCCAGATGTGATGG), *Fstl* (ACCTTCGCCTCTAACTCGCTG and CACTGGAGTCCAGGTGAGAGTC), *Gas2* (ATGGATGCCAACAAGCCTGCC) and (TCCCAGCCTCCTCCCACTCG), *Gjb3* (CCATGGACTGGAAGAAGCTC) and (TTCTCCGTGGGCCGAGCGATG), *Hoxa13* (TCGTGCGCGCAGCCTGCTTCG and GTCTGAAGGATGGGAGACGAC), *Ifit1* (GTCAAGGCAGGTTTCTGAGGA and CGATAGGCTACGACTGCATAGC), *Igfbp4* (CGGAAATCGAAGCCATCCAGG) and (GCTGGCAGGTCTCACTCTTGG), *Lamb3* (CCCACGCTGTGGAAGGGCAGG) and (CACAGTGGAGGGCAGGAGGAG), *M32486* (AGTAAGGTGTGCGCAAACAGG and TCCCGACCGTGTGTGTGGTTG), *Ngef* (TGTCCGGAAGATGAGCCGCAC and CTGGTCATGCAGCCGCTCACC), *Ppic* (CGAGGTCCCTCGGTGACGGAC and CGATGGTGCAGTCGGTGAGTG) *Tgtp* (CCACCAGATCAAGGTCACCAC and CTGTGCAATGGCTTTGGCCAG). Reactions were resolved by agarose gel electrophoresis with ethidium bromide and image analysis was performed using the Quantity One software with a Gel Doc 2000 (BioRad).

Whole mount in situ hybridization

For these experiments, the *Hoxa13* deletion and replacement with the *neo*^{r} mouse (Fromental-Ramain et al., 1996b) was crossed onto the C57BL/6J genetic background for seven generations to minimize variation in gene expression arising from background differences. Embryos were collected from matings of *Hoxa13*$^{+/-}$ mice at E11.5, E12.5, and E13.5. Embryos were staged by assigning noon of the day of vaginal plug, as E0.5. When needed, more precise staging of limb buds was done as described previously (Wanek et al., 1989). Genotyping for *Hoxa13* was done by PCR as previously reported (Post and Innis, 1999a) except for adjustment of the $MgCl_2$ concentration to 2.0 mM for the null allele. Antisense mRNA probes were transcribed as previously described for *Hoxa13* and *Hoxd13* (Post and Innis, 1999a). In situ probe templates were created to the bases from the following cDNAs cloned into pCR4 (Invitrogen): *Anxa8* (809–1821), *Col3a1* (3878–4704), *Ifit1* (13–629), *Igfbp4* (701–1128), and *Sox9* (1475–2190). *EphB3* and *Fstl* templates were kindly provided by SA Camper, and Image clones were purchased for *Fhl1* and *Gas2* (Invitrogen Clone ID: 4988977 and 4237356). DNA templates were linearized and antisense probes were transcribed using the following restriction enzymes and RNA polymerases: *Anxa8* (*Not*I and T3), *Col3a1* (*Not*I and T3), *EphB3* (*Not*I and T3), *Fhl1* (*Kpn*I and T7), *Fstl* (*Not*I and T3), *Gas2* (*Avr*II and T7), *Ifit1* (*Not*I and T3), *Igfbp4* (*Not*I and T3), and *Sox9* (*Not*I and T3). Whole-mount in situ hybridization with a single digoxygenin-labeled RNA probe was performed as previously described (Bober et al., 1994), except that BM purple (Roche) was used as the substrate for alkaline phosphatase.

Results

Construction of cells stably or transiently expressing HOXA13/EGFP and EGFP-only proteins

To avoid experimental complications caused by HOX co-expression, we exploited a cellular context free of HOX paralog group 13 activity in order to identify candidate HOXA13 regulated genes. Ecotropic retroviral packaging cells were created using the GP + E86 cell line, which was derived from mouse NIH 3T3 embryonic fibroblast cells (Markowitz et al., 1990), and which do not express HOXA13 or HOXD13. HOXA13/EGFP and EGFP-only viral packaging cells were created using MoMLV-based retroviral vectors modified with a bicistronic *Hoxa13*-IRES-EGFP expression cassette and control cells that contain only the IRES-EGFP element (Fig. 1A). Retroviral vector DNA was transfected into amphotropic Phoenix-A cells to produce retroviral-containing supernatants. These viral supernatants were then used to transinfect the GP + E86 cells. The infected GP + E86 cells expressing the *Hox* and/or GFP gene(s) were separated away from the untransduced cells by GFP-based FACS (data not shown) to create a heterogeneous population of ecotropic viral producer cells, hereafter referred to as stable-expressing cells. After this enrichment for cells expressing the transgene(s), Western analysis demonstrated that only the HOXA13/EGFP stable-expressing cells expressed HOXA13 (Fig. 1B). In addition to stable expression of these gene(s), these cells produce supernatants containing competent ecotropic retrovirus that often have a high viral titer and can be used for efficient infection in transient infection/expression studies. Supernatants from these cells were used to transinfect two murine embryonic fibroblast

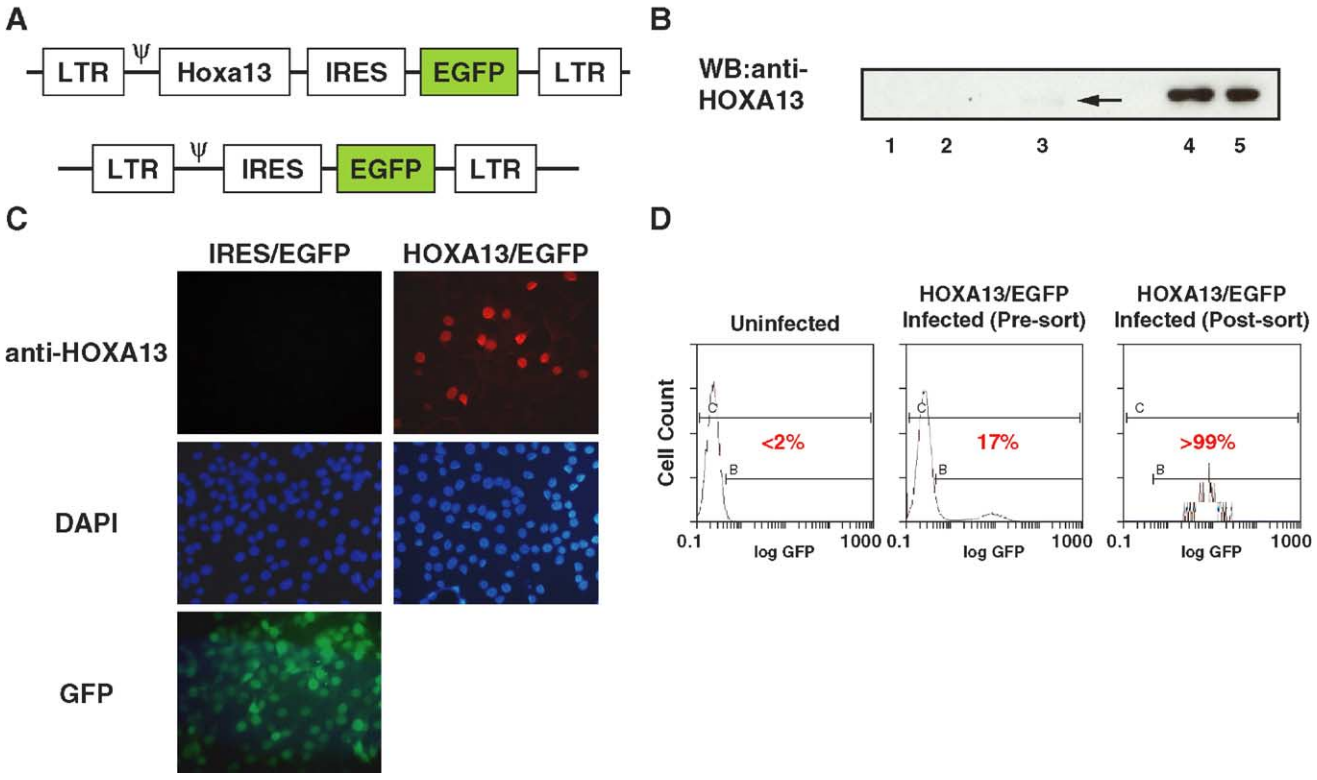

Fig. 1. Creation of cells expressing either HOXA13/EGFP or EGFP-only. (A) Stable expressing retroviral producing cell lines were created using MoMLV-based retroviral vectors modified with a bicistronic *Hoxa13*-IRES-EGFP expression cassette and only with the IRES-EGFP element. (B) Western blot demonstrates HOXA13 expression in the HOXA13/EGFP but not the control EGFP-only retroviral producer cells. Equivalent amounts of protein were loaded in each lane. (1) EGFP-only stable-expressing control cells; (2) EGFP-only transinfected 10T1/2 cells; (3, arrow) minimal expression of HOXA13 is detected in the transinfected 10T1/2 cells; (4) HOXA13 expression in the stable-expressing cells; (5) expression of HOXA13 in the MLB13-myc cell line derived from mouse limb buds. HOXA13 protein expression in our stable-expressing cell line is comparable to immortalized limb derived cells. (C) Immunocytochemistry indicates expression of HOXA13 in transinfected NIH 3T3 cells using viral supernatants from HOXA13/EGFP but not the EGFP-only viral producer cells. DAPI staining demonstrates that HOXA13 is localized to the nucleus. GFP expression shows successful transinfection by EGFP-only retrovirus. (D) GFP-based FACS can enrich for near-pure cell populations expressing the transgene(s). HOX translation is initiated on a bicistronic message; EGFP expression, and by inference HOXA13, is consistently ~3-fold lower in the HOXA13-expressing cells.

cell lines, NIH 3T3 and C3H 10T1/2, which like the GP + E86 cells, do not express either HOXA13 or HOXD13 in their untransduced state (data not shown). The goal of this infection was to test downstream gene expression changes 48 h after expression of HOXA13. Immunocytochemistry performed 48 h post-infection demonstrated expression and nuclear localization of HOXA13 in the cells infected by the HOXA13/EGFP virus, but not in those infected by the control virus (Fig. 1C). In these experiments, the efficiency of transinfection ranged from 10–80%, and GFP-based FACS was used to enrich for a near homogenous population of infected cells expressing the transgene(s) (Fig. 1D). RNA (data not shown) and protein analysis (Fig. 1B) showed significantly lower expression of HOXA13 in the transinfected cells at 48 h post infection compared to the stable-expressing cells. In addition, HOXA13 protein expression in the HOXA13 stable-expressing cell line was comparable to immortalized limb derived cells (Rosen et al., 1994). Furthermore, we have also observed similar levels of HOXA13 protein in comparable amounts of limb bud protein preparations, suggesting that expression in our stable-expressing cells is near physiological levels.

Gene expression changes unique to HOXA13/EGFP-expressing cells

To identify candidate HOXA13 downstream genes, transcriptional profiles were generated using murine U74Av2 oligonucleotide arrays containing 12,488 probe sets that interrogate expression levels of ~9000 distinct genes. Total cellular RNA was prepared from two independent samples of stable expressing HOXA13/EGFP and EGFP-only cells, and two samples each from FACS-enriched C3H 10T1/2 and NIH 3T3 cells 48 h following transinfection with either HOXA13/EGFP or EGFP-only retrovirus. These 12 RNA samples were analyzed using 12 separate arrays. Table 1 summarizes the number of probe sets identified with reproducible, significant ($P < 0.01$) expression changes for comparisons between HOXA13-expressing and non-expressing control cells. Of the 12,488 probe sets on the microarray, the stable-expressing cells

Table 1
Reproducible expression differences between *Hoxa13*-expressing and non-expressing cells

Cells	*P* value < 0.01 (expected by chance)	*P* value < 0.01 and fold change > 1.75
Stable-expressing GP + E86 (3T3)	399 (125)	73
C3H 10T1/2	119 (125)	4
NIH 3T3	190 (125)	12

comparison reported the greatest number of significant differences ($P < 0.01$), with 399. For the transinfected cells, 119 and 190 probe sets showed significant differences for the 10T1/2 and 3T3 cells, respectively. For each comparison, assuming a false-positive rate of 1%, we would have expected by chance to observe roughly 125 probe sets meeting this significance level. To reduce the number of false-positives, we added the co-requirement of a >1.75-fold difference in mean expression levels for each probe set between the HOXA13-expressing and non-expressing cells. For the stable-expressing cell comparison, 73 probe sets qualified, compared to 4 and 12 for 10T1/2 and 3T3 cells, respectively. The only qualifying probe set in common between the stable-expressing cells and either of the transinfected cells was that for *Hoxa13* in the 3T3 cells. The relative paucity of probe sets with significant differences in expression for the transinfected cells, may be explained by the lower level of HOXA13 expression in these populations (Fig. 1B, compare lanes 3 and 4). The low level of RNA expression for *Hoxa13* in the transinfected cells, as determined by the microarray, is consistent with the low protein level. Despite this, the microarray data from these transinfected cells was useful in estimating the variance in gene expression between replicate stable-expressing samples (see Material and methods).

We elected to focus our attention on the gene expression changes in the stable-expressing cells. These gene expression changes were derived from two replicate experiments. Permutation testing was performed in which (one or more) pairs of samples were reversed in order to estimate the false-positive rate (Tusher et al., 2001). Considering only those permuted data sets where a pair of stable-expressing cells were reversed, we obtained an average of only 12 probe sets meeting the criteria of $P < 0.01$ and a fold change (FC) > 1.75 (either up or down) where we obtained 73 from the actual data. Thus, permutation testing suggested that 12 of 73 could be false positives. Thus, ~84% of the changes are more likely to have resulted from HOXA13 expression.

Of the 73 qualifying probe sets, 54 probe sets representing 50 different genes had higher expression in the HOXA13 stable-expressing cells (Table 2). Gene expression differences ranged between +30.75 for *Fhl1* and +1.76 for *Idb1*. Three probe sets for *Aldh2* and a second probe set for both *Col3a1* and *Fhl1* were in this group of upregulated probe sets. Among these 50 genes are *Anxa8* and *M32486* genes that have been identified in previous studies (Table 5) as putative HOXA13-regulated targets (Zhao and Potter, 2001). 19 probe sets, representing 18 different genes, were identified as having significantly lower expression in the HOXA13 stable-expressing cells (Table 3). The fold changes within this group lie between −5.88 for *Ngef* and −1.75 for *Mox2*. One of these 18 genes, *Casp8ap2* was previously shown to be upregulated by *Hoxb4* (Morgan et al., 2004).

Functional categories of genes overrepresented in HOXA13/EGFP-expressing cells

To determine the categories of genes regulated by HOXA13, we tested whether any Gene Ontology (GO) terms are overrepresented for the genes found as increased in the HOXA13/EGFP-expressing cells compared to the remaining genes assayed by the microarrays. Of the 399 probe sets with expression differences with a significance of $P < 0.01$, we confined our analysis to those that met the corequirement of having a FC > 1.0 (upregulated only) in the HOXA13-expressing cells because this produced the most biologically interesting data with the strongest statistical support. This resulted in 208 qualifying probe sets that were further reduced to 181 distinct genes for which there are LocusLink identifiers and gene symbols available. The remaining probe sets on the array correspond to 8245 distinct genes with LocusLink identifiers. Using publicly available software (Creighton et al., 2003) we found 11 GO terms to be significantly enriched in this set of upregulated genes ($P < 0.001$, Table 4). In order to assess the chance that selection of these specific GO terms was a false-positive result, we performed Monte Carlo simulations in which 100 random sets of 181 gene symbols were chosen from the arrays. Among these 100 data sets, we obtained an average of only 0.8 GO terms with $P < 0.001$, and the maximum number of terms in any single data set was 5. Data for alternative analyses with different criteria for expression differences is available at http://dot.ped.med.umich.edu:2000/pub/hox/index.html. In general, these comparisons support the analysis above.

Validation of microarray identified expression differences

To validate the expression differences identified by the microarray, we adapted a semi-quantitative RT-PCR (SQ RT-PCR) method (Baigent and Lowry, 2000). RNA from a preparation used for the microarray analysis and a third independent preparation were used to verify the expression differences for a subset of the 68 candidate HOXA13 regulated genes. Equal amounts of input RNA from both the stable HOXA13-expressing (+) and non-expressing (−) cells were compared over serial dilutions ranging between 10,000 and 38 pg total RNA (Fig. 2). For each RNA dilution, all other variables were held constant so that the final signal was proportional to the amount of input RNA. As a positive control, *Hoxa13* expression was analyzed first to demonstrate the ability of the assay to show differences in expression between the RNA sources. Consistent with the

Table 2
Genes reproducibly upregulated at least 1.75-fold in stable *Hoxa13*-expressing cells

Gene symbol	Mean fold change	*P* value	Description	NCBI locus link
Membrane/cytoskeleton				
Enpp2	10.81	0.0028	ectonucleotide pyrophosphatase/phosphodiesterase 2	18606
M32486	5.50	0.0000	Mouse 19.5 mRNA	56277
Gjb3	5.46	0.0058	gap junction membrane channel protein beta 3	14620
Itpr5	3.35	0.0005	inositol 1,4,5-triphosphate receptor 5	16442
Anxa8	3.26	0.0045	annexin A8	11752
Shrm	2.86	0.0027	shroom	27428
Blnk	2.81	0.0005	B-cell linker (lymphocyte antigen 57)	17060
Ly6c	2.49	0.0004	expressed sequence AA682074	17067
Syt8	2.48	0.0002	synaptotagmin 8	55925
Myo7a	2.20	0.0060	myosin VIIa	17921
Ly6a	2.17	0.0007	lymphocyte antigen 6 complex, locus A	110454
Synpo	2.02	0.0016	expressed sequence AW046661	104027
Extl3	1.93	0.0014	exostoses (multiple)-like 3	54616
Copz2	1.86	0.0095	coatomer protein complex, subunit zeta 2	56358
EphB3	1.85	0.0044	Eph receptor B3	13845
Ghr	1.82	0.0075	growth hormone receptor	14600
Ank3	1.78	0.0003	ankyrin 3, epithelial	11735
Metabolism/enzymes				
Fabp4	3.76	0.0010	fatty acid binding protein 4, adipocyte	11770
Aldh2[a]	3.52	0.0007	aldehyde dehydrogenase 2, mitochondrial	11669
Aldh3a1	2.67	0.0012	aldehyde dehydrogenase family 3, subfamily A1	11670
Gstt1	2.58	0.0015	glutathione *S*-transferase, theta 1	14871
Lip1	2.16	0.0030	lysosomal acid lipase 1	16889
Ptgis	1.80	0.0034	prostaglandin I2 (prostacyclin) synthase	19223
P4ha2	1.80	0.0015	procollagen-proline, 2-oxoglutarate 4-dioxygenase	18452
Nuclear				
Fhl1[b]	30.75	0.0005	four and a half LIM domains 1	14199
Hoxa13	20.70	0.0024	homeo box A13	15398
Ebf3	2.13	0.0064	early B-cell factor 3	13593
Tcf3	2.01	0.0052	transcription factor 3	21415
Idb1	1.76	0.0043	inhibitor of DNA binding 1	15901
Secreted/extracellular matrix				
Fbn1	5.03	0.0000	fibrillin 1	14118
Fstl	4.61	0.0001	follistatin-like	14314
Igfbp4	2.91	0.0006	insulin-like growth factor binding protein 4	16010
Lamb3	2.83	0.0012	laminin, beta 3	16780
Col3a1[b]	2.77	0.0060	procollagen, type III, alpha 1	12825
Adm	2.75	0.0004	adrenomedullin	11535
S100a13	2.72	0.0004	S100 calcium binding protein A13	20196
Mfap5	2.55	0.0010	microfibrillar associated protein 5	50530
Col5a2	1.99	0.0006	procollagen, type V, alpha 2	12832
Col4a2	1.86	0.0048	procollagen, type IV, alpha 2	12827
Signal transduction/growth control				
Tgtp	3.32	0.0003	T-cell specific GTPase	21822
Gas2	2.68	0.0027	growth arrest specific 2	14453
Adcy7	2.04	0.0040	adenylate cyclase 7	11513
Function not elucidated				
Ifit1	4.37	0.0055	interferon-induced protein with tetratricopeptide repeats 1	15957
AA407270	2.58	0.0097	expressed sequence AA407270	270174
No Title	2.37	0.0022	ESTs	381697
BC028953	2.33	0.0013	DNA segment, Chr 14, ERATO Doi 231, expressed	210925
St5	2.10	0.0082	RIKEN cDNA 2010004M01 gene	76954
Aim1	1.98	0.0004	absent in melanoma 1	11630
1700020M16Rik	1.87	0.0061	RIKEN cDNA 1700020M16 gene	71843
No Title	1.81	0.0074	expressed sequence AI413214	66180

[a] Indicates that two additional probe sets identified the gene as being upregulated in the Hoxa13 expressing cells.
[b] Indicates that a second probe set identified the gene as being upregulated in the Hoxa13 expressing cells.

Table 3
Genes reproducibly downregulated at least 1.75-fold in stable Hoxa13-expressing cells

Gene symbol	Mean fold change	*P* value	Description	NCBI locus link
Membrane/cytoskeleton				
Klra4	−1.92	0.0074	killer cell lectin-like receptor, subfamily A, member 4	16635
Mox2	−1.75	0.0073	antigen identified by monoclonal antibody MRC OX-2	17470
Nuclear				
Srrm1	−2.44	0.0099	serine/arginine repetitive matrix 1	51796
Brul4	−2.33	0.0052	Brunol4: bruno-like 4, RNA binding protein (*Drosophila*)	108013
Rag1	−1.96	0.0071	recombination activating gene 1	19373
Secreted/extracellular matrix				
Tpbpb[a]	−2.78	0.0012	trophoblast specific protein beta	116913
Ngfb	−1.79	0.0043	nerve growth factor, beta	18049
Signal transduction/growth control				
Ngef	−5.88	0.0015	neuronal guanine nucleotide exchange factor	53972
Ramp3	−2.38	0.0029	receptor (calcitonin) activity modifying protein 3	56089
Rgs2	−2.17	0.0015	regulator of G-protein signaling 2	19735
Casp8ap2	−1.89	0.0009	caspase 8 associated protein 2 (FLASH)	26885
Function not elucidated				
4930553M18Rik	−2.38	0.0093	RIKEN cDNA 4930553M18 gene	75316
No Title	−2.17	0.0040	AK011460.1	–
1500034J01Rik	−2.04	0.0002	RIKEN cDNA 1500034J01 gene	66498
5730408K05Rik	−1.96	0.0077	RIKEN cDNA 5730408K05 gene	67531
Fin15	−1.92	0.0053	fibroblast growth factor inducible 15	14210
2310005N03Rik	−1.89	0.0026	RIKEN cDNA 2310005N03 gene	66359
4930553M18Rik	−1.82	0.0012	RIKEN cDNA 4930553M18 gene	75316

[a] Indicates that a second probe set identified the gene as being downregulated in the Hoxa13 expressing cells.

Table 4
Significantly enriched ($P < 0.001$) Gene Ontology (GO) terms assigned to upregulated genes

GO category	GO term	Count in 181 upregulated genes with $P < 0.01$	Count in remaining 8051 genes	Fold enrichment of term[a]	*P* value, one-sided Fisher's Exact Test	Upregulated genes with this term
Cellular component	extracellular matrix	13	134	4.4	0.000007	Col1a1, Col3a1, Col4a1, Col4a2, Col5a2, Fbln2, Fbn1, Lamb2, Lamb3, Mfap5, Mmp14, Smoc, Sparc
Molecular function	extracellular matrix structural constituent	7	36	8.9	0.000011	Col1a1, Col3a1, Col4a1, Col4a2, Col5a2, Lamb2, Lamb3
Cellular component	basement membrane	6	26	10.5	0.000017	Col4a1, Col4a2, Lamb2, Lamb3, Smoc1, Sparc
Cellular component	clathrin vesicle coat	4	11	16.6	0.000066	Ap3s1, Ap3s2, Copz1, Copz2
Cellular component	coated vesicle	6	41	6.7	0.000245	Ap3s1, Ap3s2, Copz1, Copz2, Sec23a, Syt8
Cellular component	collagen	5	27	8.4	0.000263	Col1a1, Col3a1, Col4a1, Col4a2, Col5a2
Molecular function	extracellular matrix, structural constituent, conferring tensile strength	5	27	8.4	0.000263	Col1a1, Col3a1, Col4a1, Col4a2, Col5a2
Biological process	protein transport	16	276	2.6	0.000359	Ap3s1, Ap3s2, Arfgap3, Bcap31, Copz1, Copz2, Ctsb, Gabarap, Ghr, Lman1, Lrp10, Rab25, Rin2, Sec22l1, Sec23a, Snap23a
Cellular component	Golgi membrane	4	19	9.6	0.000673	Bcap31, Man2a1, Sec22l1, Sec23a
Biological process	intracellular protein transport	13	214	2.8	0.000837	Ap3s1, Ap3s2, Arfgap3, Bcap31, Copz1, Copz2, Ctsb, Gabarap1, Lman1, Rab25, Sec22l1, Sec23a, Snap23
Cellular component	clathrin-coated vessicle	5	35	6.5	0.000918	Ap3s1, Ap3s2, Copz1, Copz2, Syt8

Only distinct genes that had LocusLink indentifiers were used in statistical tests.
[a] Ratio of (Count in 181/181)/(Count in 8051/8245).

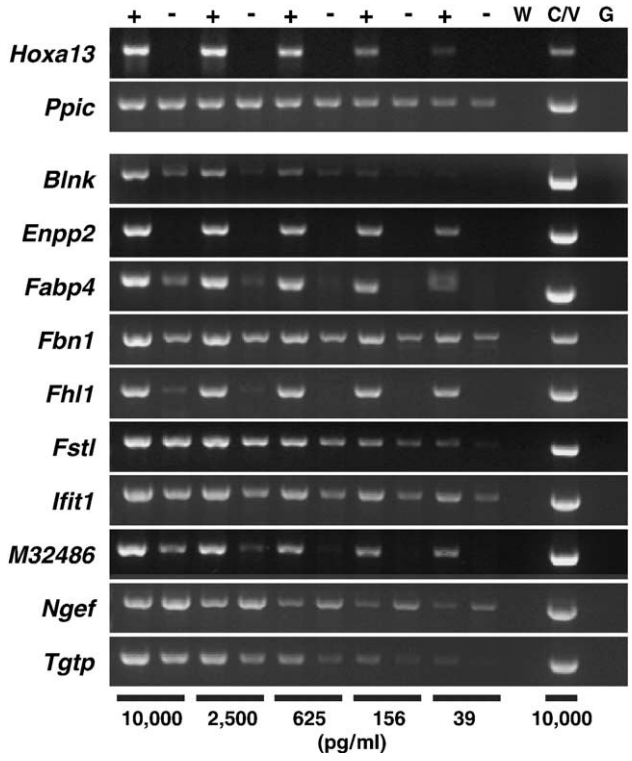

Fig. 2. Semi-quantitative RT-PCR validates expression differences for 10 candidate HOXA13 downstream genes. RNA from stable HOXA13/EGFP (+) and EGFP-only (−) cells were compared across serial dilutions of input RNA ranging from 10,000 to 39 pg/μl. *Hoxa13* expression was tested as a positive control and *Ppic* as a negative control of differential expression. Consistent with microarray fold changes, of the 10 genes examined, 9 have reproducibly higher expression in the HOXA13/EGFP cells, and 1 (*Ngef*) has lower. Control reactions were included using water (W), RNA from caudal female reproductive tracts (C/V), and genomic DNA (G).

microarray data, the assay reported no detectable difference in the expression of *Ppic*, a housekeeping gene unlikely to be regulated by HOXA13. Using this method, 11 of the most highly differentially expressed 68 candidate downstream genes were tested. For 10 of the 11, the direction of expression change was confirmed. Genes such as *Fhl1*, *M32486*, and *Enpp2*, which were identified by the microarray to have large fold changes, were shown to have dramatic changes in expression by SQ RT-PCR. In our experience, this method repeatedly demonstrates accurate directional changes in expression but can fail to detect changes for targets with smaller fold changes, particularly those with high basal expression in the cell line. For example, *Fstl* was determined by the array to be expressed 4.61-fold higher in the HOXA13 stably expressing cells; by SQ RT-PCR, at higher levels of input RNA, only a subtle difference in expression was detected. As the input RNA was reduced, the difference in expression became more apparent. This may explain why the SQ RT-PCR failed to detect a difference in the expression of *Anxa8*, a gene with a smaller FC in expression (+3.26-fold) and is also highly expressed in the EGFP-only cells (data not shown). To further support the validity of these gene expression differences, 7 of these 10 genes were tested by SQ RT-PCR in a third independent preparation of RNA and shown to have similar expression differences (data not shown).

Candidate downstream target gene expression in vivo

To determine whether some of these genes are normally expressed in tissues that express HOXA13, and therefore present an opportunity for regulation, we performed RT-PCR on a subset of 16 candidates for expression in the developing distal (autopod) limb bud (LB) and the caudal region of the female reproductive tract consisting of the cervix and vagina (C/V) (Fig. 3), two regions of known *Hoxa13* expression and function (Fromental-Ramain et al., 1996b; Taylor et al., 1997; Warot et al., 1997). Expression was demonstrated for each of the tested genes in at least one of the two RNA sources, with *Anxa8*, *Col3a1*, *Enpp2*, *Fbn1*, *Fhl1*, *Fstl*, *Gas2*, *Ifit1*, *Ifgfbp4*, and *M32486* expressed highly in both. Expression of *Blnk*, *Fabp4*, *Gjb3*, *Lamb3*, *Ngef*, and *Tgtp* was faint in the LB compared to the C/V.

To determine whether any of the limb bud expressed candidates have in vivo expression patterns that overlap with *Hoxa13*, whole mount in situ hybridization was performed using forelimbs and hindlimbs (Fig. 4). Between early (stage 7) and mid (stage 8) E12.5 limb buds, *Hoxa13* expression changes from being broadly expressed across the entire anteroposterior axis of the distal autopod (Fig. 4B), to being excluded from the prechondrogenic cartilage condensations of the developing digits while maintaining expression within the interdigital mesenchyme (ID, Fig. 4C) (Suzuki and Kuroiwa, 2002). Expression in the ID can be seen clearly for *Anxa8*, *Fstl*, and *Igfbp4* (Figs. 4E,I,L). The expression of *Col3a1*, *EphB3*, *Fhl1*, *Gas2*, and *Ifit1* (Figs. 4F,G,H,J,K) also appear expressed in the ID, however the signal was much lower, at least with the probes and conditions used here. Previous studies have more clearly demonstrated the IDM-restricted expression of *EphB3* and *Gas2* (Compagni et al., 2003; Lee et al., 1999). *Enpp2*, also known as autotaxin, has been shown to be expressed around the developing digits in precartilaginous condensations and joint regions beginning in the limbs at ~E14.5 (Bachner et al., 1998, 1999). Our efforts to examine in situ expression of this gene in limb buds at E12.5 were unsuccessful, despite the positive signal by RT-PCR (Fig. 3). The distal joint defects in *Hoxa13* mutant mice and the fact that *Enpp2* is downstream in BMP2 metabolism makes *Enpp2* a strong candidate for HOXA13 regulation. Together, the expression data from both RT-PCR and in situ hybridization demonstrates coexpression for many candidate downstream genes and *Hoxa13* in the caudal female reproductive tract and/or the developing limb buds of wild type mice.

Misregulation of Igfbp4 and Fstl in Hoxa13$^{-/-}$ embryos

Using RNA from E12.5 *Hoxa13*$^{+/+}$ and *Hoxa13*$^{-/-}$ distal limb buds, no observable changes in expression were

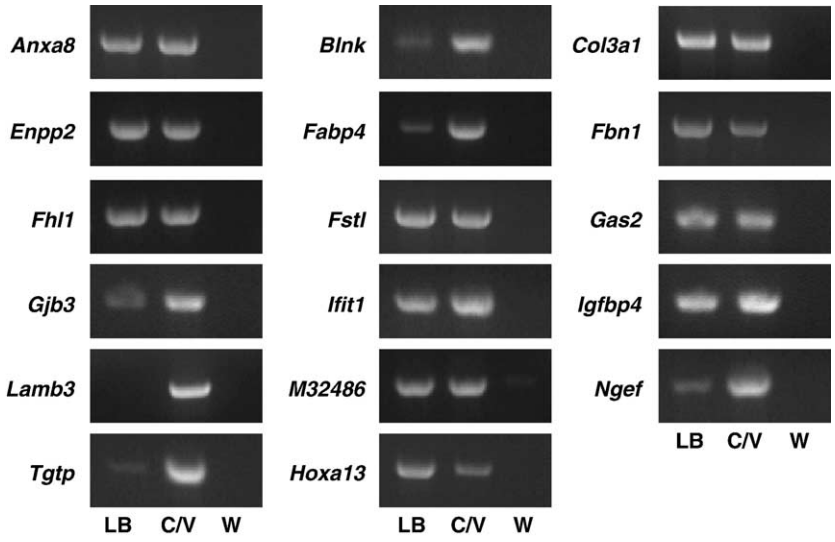

Fig. 3. Expression analysis for 16 of the 68 candidate HOXA13 downstream target genes in tissues of known *Hoxa13* expression. RT-PCR was performed using RNA from developing distal limb buds (LB) and the caudal female reproductive tract (C/V). Control reactions that included water (W) instead of input RNA were also performed for each gene.

observed by SQ RT-PCR for *Enpp2*, *Fhl1*, *Fstl*, *Igfbp4* or *M32486* (data not shown), candidates with some of the largest reported expression changes in the in vitro assay (Table 2). This could be explained by the lack of strict quantitative assay capabilities, pooling of the samples which might have raised the contribution of cells normally not

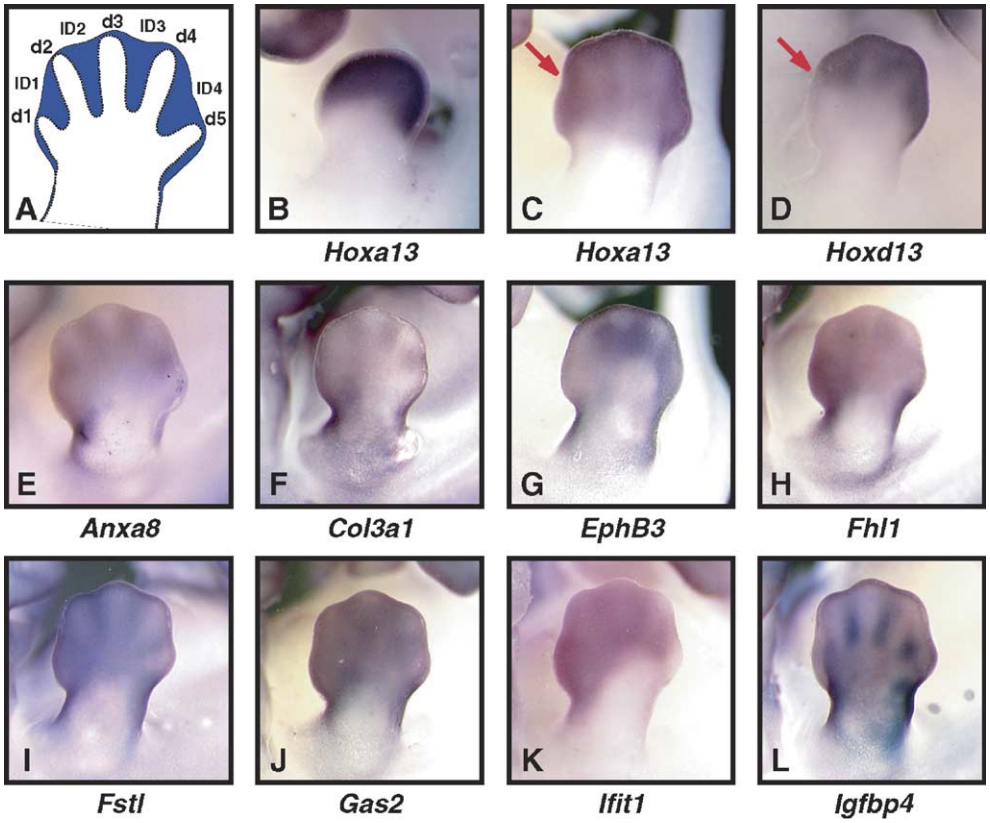

Fig. 4. Interdigital limb bud expression of candidate HOXA13 target genes. Whole mount in situ hybridization analysis for limb bud RNA expression. (A) Schematic of an E12.5 limb bud indicating the position of anterior digit 1 (d1) and the progression to posterior-most digit 5 (d5). The mesenchyme surrounding the digital condensations are in purple, with interdigital regions specified (ID1–4). (B) *Hoxa13* expression at E11.5 is throughout the distal autopod. (C) At E12.5, *Hoxa13* expression becomes restricted to the interdigital mesenchyme. (D) *Hoxd13* expression largely overlaps that of *Hoxa13*, but the expression does not extend as far anterior (compare red arrows) as ID1 and d1. Coincident interdigital expression is observed for (E) *Anxa8*, (F) *Col3a1*, (G) *EphB3*, (H) *Fhl1*, (I) *Fstl*, (J) *Gas2*, (K) *Ifit1*, and (L) *Igfbp4* at E12.5. Images (B, C, and G) are of hindlimbs, and all others are forelimbs.

expressing *Hoxa13*, use of only one limb stage that may not have been optimal for seeing an expression difference, or could result from the remaining expression of paralog *Hoxd13* and several nonparalogous *Hox* genes in the mutant limb buds. This result would not preclude a change in the distribution or relative abundance of candidate expression that might be visualized in mutants using whole-mount in situ hybridization.

To test whether *Hoxa13* is required for ID limb expression of selected candidate downstream regulated genes, we compared expression in *Hoxa13*$^{+/+}$ and *Hoxa13*$^{-/-}$ embryo limb buds by whole mount in situ hybridization in several limb stages (Figs. 5 and 6). For *Igfbp4*, in both wild type and mutant embryos at early E12.5 (stage 7), there is high expression in the proximal forelimb bud and to a lesser degree evenly throughout the distal autopod (Figs. 5A,D). At mid E12.5 (stage 8), the proximal expression of *Igfbp4* remains in both wild type and mutant forelimb buds, however ID expression turns on in the wild type forelimb buds (Fig. 5B), while expression in the mutants appears much weaker in several ID regions (Fig. 5E). By late E12.5 (stage 9), the expression of *Igfbp4* in wild type limb buds is strongest in ID1 and ID4, and weaker in ID2 and ID3. In mutants at the same stage, *Igfbp4* is expressed in ID2–4 (albeit weaker in ID4), but not in ID1 (Fig. 5F).

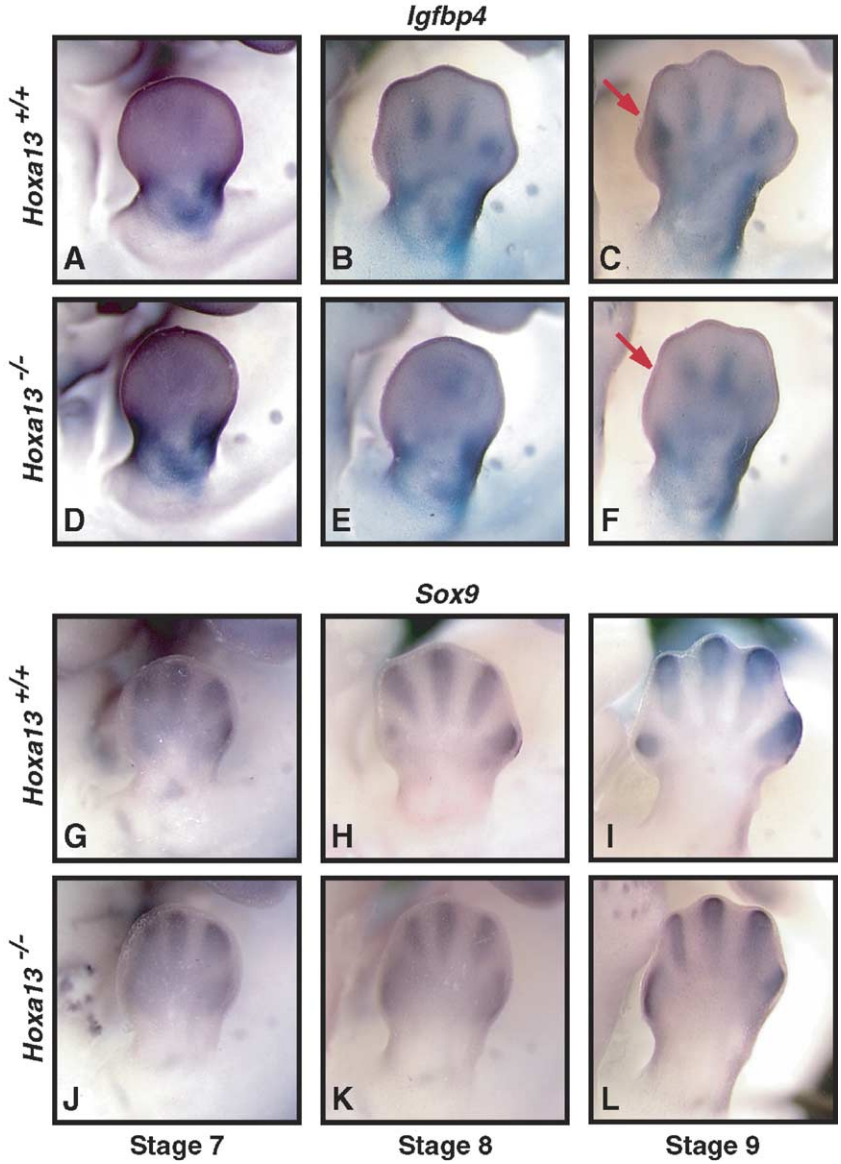

Fig. 5. Misregulation of *Igfbp4* expression in *Hoxa13*$^{-/-}$ limb buds. Comparison of *Igfbp4* expression in forelimbs of (A–C) *Hoxa13*$^{+/+}$ and (D–F) *Hoxa13*$^{-/-}$ embryos between E12.5 stages 7 and 9. (A) At stage 7, *Igfbp4* is expressed primarily in the proximal limb bud, with interdigital expression apparent at (B) stage 8 and persisting through (C) stage 9. (D–F) While proximal expression is unaltered in the mutant limb buds, at stage 8, a weaker and disorganized expression pattern is seen in the (E) mutant limb buds compared to the ID2–4 expression in (B) wild type littermates. At stage 9, ID1 expression is absent in (F) mutant limb buds but not (C) wild type littermates (compare red arrows). *Sox9* expression in forelimbs of (G–I) *Hoxa13*$^{-/-}$ and (J–L) *Hoxa13*$^{+/+}$ littermates demonstrates that mutant limb buds are at comparable developmental stages.

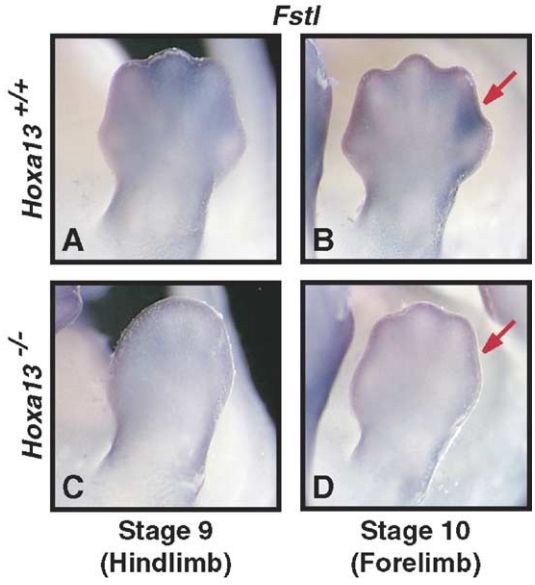

Fig. 6. *Fstl* expression is misregulated in *Hoxa13*$^{-/-}$ embryos. (A) In late E12.5 limb buds (stage 9, hindlimbs) of *Hoxa13*$^{+/+}$ embryos, *Fstl* expression is higher in ID2 and ID3. (B) At early E13.5 (stage 10, forelimbs) limb buds, *Fstl* is highly expressed in the posterior ID4 relative to ID1-3. In *Hoxa13*$^{-/-}$ limb buds, *Fstl* expression is reduced at both (C) stage 9 and (D) stage 10, most notably in the posterior ID4 at stage 10 (compare red arrows).

In the course of experimentation, great care was taken in the proper staging of mutant and wild type limb buds to be confident that the presented differences in expression are due to the loss of *Hoxa13* rather than a result of delayed development or faulty staging. The misshapen appearance of the *Hoxa13* mutant limbs results from hypoplasia of the developing digits and is not an indication of inappropriate staging or absence of tissue in the mutant limbs (Fromental-Ramain et al., 1996b). *Sox9* expression at stages 8 and 9 reveals that the prechondrogenic condensations have similarly developed in the *Hoxa13*$^{-/-}$ embryos compared to that seen in the wild type embryos (compare Figs. 5H,K). This supports our conclusion that the stages presented are indeed comparable and that subtle morphologic differences result from hypoplasia of digits 1, 2, and 5 rather than a developmental delay (Figs. 5G–L). Further examination of a more advanced stage of *Hoxa13*$^{-/-}$ limbs in Fig. 5F, by comparison with Fig. 5B, shows clearly reduced levels of *Igfbp4* staining, and this is supported by the more advanced Sox9 expression pattern for mutants shown in Fig. 5L. These comparisons were repeated with five additional mutant embryos, and a consistent defect in *Igfbp4* expression was observed. Additionally, similar differences were observed in the hindlimbs of *Hoxa13*$^{-/-}$ (not shown).

The expression of *Fstl* was also analyzed. At late E12.5 in *Hoxa13*$^{+/+}$ embryos (stage 9), *Fstl* is expressed in ID2–4 with the level in ID2 and ID3 greater than in ID4 (Fig. 6A). The expression of *Fstl* at early E13.5 (stage 10) is decreased in ID2 and ID3 and increased in ID4 (Fig. 6B). The expression of *Fstl* in *Hoxa13*$^{-/-}$ limb buds (Figs. 6C,D) is attenuated compared to that of the wild type littermates. A consistent decrease in *Fstl* expression was observed in replicate experiments in the *Hoxa13*$^{-/-}$ embryos. In our experience, the degree of loss is variable, however ID4 expression was always reduced. Together these data demonstrate a genetic requirement for *Hoxa13* for the proper expression of *Igfbp4* and *Fstl* in the interdigital mesenchyme of developing limb buds.

Paralog and non-paralog target gene regulatory capabilities

To test whether other HOX group 13 proteins regulate the expression of candidate HOXA13 downstream genes, we performed a transient transfection assay with HOXA13 and HOXD13 in the control EGFP-only cells. To simplify the analysis, we looked at *Blnk*. We repeatedly demonstrated by SQ RT-PCR that the expression of *Blnk* was upregulated upon the transfection of either paralog (Fig. 7A). This

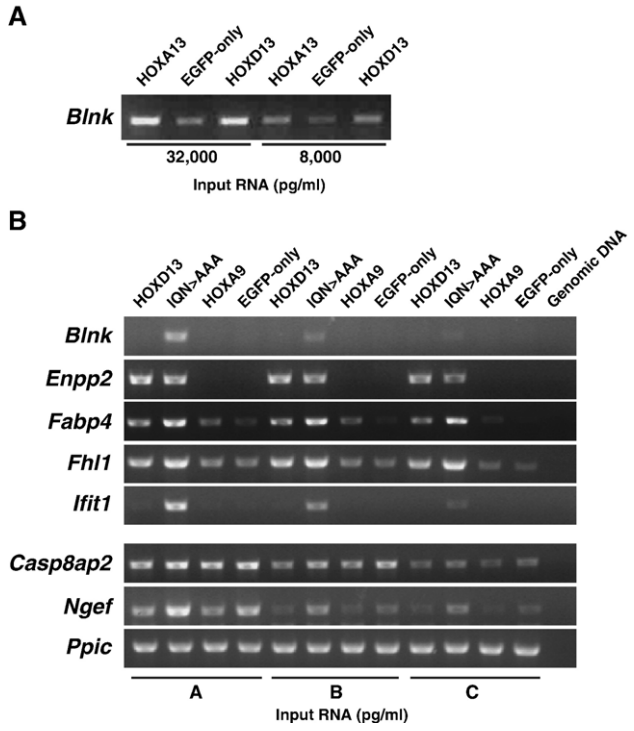

Fig. 7. Coregulation of candidate HOXA13 downstream genes by other HOX proteins, and a variable requirement for monomeric DNA-binding capability. Semi-quantitative RT-PCR comparison of gene expression in (A) EGFP-only cells after transient expression of HOXA13 and HOXD13, and (B) stable-expressing cells. (A) Transient expression of HOXD13, like HOXA13, increases the expression of *Blnk*. (B) The expression of *Enpp2*, *Fabp4*, and *Fhl1* are increased in cell lines expressing HOXD13 or monomeric DNA-binding mutant HOXD13$^{IQN > AAA}$, but not in those expressing HOXA9. *Blnk* and *Ifit1* expression is increased only in HOXD13$^{IQN > AAA}$ cells. *Casp8ap2* and *Ngef* have reduced expression in cells expressing either HOXD13 or HOXA9, but not in the cells expressing HOXD13$^{IQN > AAA}$. The amount of input RNA used for A, B, and C was 10,000, 2500, and 625 pg/μl for *Blnk*, *Casp8ap2*, *Enpp2*, *Fabp4*, *Fhl1*, *Ppic*, and 625, 156, and 39 pg/μl for *Ifit1* and *Ngef*, respectively.

encouraged us to further explore the effect of paralogous as well as nonparalogous HOX protein expression on a larger set of candidate targets in stable cell lines, created as for HOXA13, where we could harvest cell populations with more homogeneous expression. Western blot analysis demonstrated comparable expression of HOXA9 to that of HOXA13, but much lower (at least 10-fold) levels of HOXD13 were observed (data not shown). Expression was tested by SQ RT-PCR for genes upregulated in the HOXA13-expressing cells in comparison to the EGFP-only cells. Increased expression was observed for *Enpp2*, *Fabp4* and *Fhl1* in HOXD13-, but not HOXA9-, expressing cells (Fig. 7B). *Blnk* and *Ifit1* showed no increase in either the HOXD13- or HOXA9-expressing cells. Given that *Blnk* had increased expression after transient HOXD13 expression, it is likely that the lack of a response may be due to low HOXD13 levels in this population of HOXD13 stable-expressing cells. Since the SQ RT-PCR assay is not as useful for detecting changes in expression of genes that are initially highly expressed in the EGFP-only cells, we did not test the expression of *Fstl* and *Igfbp4*. *Ngef* and *Casp8ap2* had lower expression levels in the HOXA13/EGFP-expressing cells (*Ngef*, Fig. 2; *Casp8ap2* decreased 1.3-fold, not shown). HOXD13- and HOXA9-expressing cells also had reduced expression of *Ngef* and *Casp8ap2* (Fig. 7B) by a magnitude consistent with that observed by microarray for the HOXA13/EGFP-expressing cells (Table 3). Thus, these results demonstrate that group 13 HOX proteins were capable of upregulating a subset of the genes that HOXA9 could not, implying a paralog-specific regulatory effect. However, the repression of *Ngef* and *Casp8ap2* was a shared property.

Downstream target gene regulation by HOXD13 monomeric DNA-binding mutant

Previous studies have demonstrated the importance of homeodomain (HD) residues 47, 50, and 51, that make direct contact with the DNA (Gehring et al., 1994b). The conversion of all of these residues (I, Q, N) to alanine creates a protein unable to effectively bind a group 13 HD binding site as a monomer in vitro (Caronia et al., 2003). To test whether monomeric DNA-binding capability is a requirement for target gene regulation, we created cells stably expressing HOXD13$^{IQN > AAA}$ (as done for *Hoxa13*, *Hoxd13* and *Hoxa9*). Western blot analysis demonstrated robust protein expression perhaps greater than for both the HOXA9- and HOXD13-expressing cells (data not shown). RNA prepared from these cells was analyzed by SQ RT-PCR. Surprisingly, HOXD13$^{IQN > AAA}$ was able to upregulate the expression of *Enpp2*, *Fabp4* and *Fhl1*, comparable to that of wild type HOXD13 (Fig. 7B). Also, *Blnk* and *Ifit1* were upregulated in cells expressing HOXD13$^{IQN > AAA}$, but not in those expressing wild type HOXD13 or HOXA9. We ruled out the possibility that the observed expression changes were secondary to HOXD13$^{IQN > AAA}$ upregulating the endogenous expression of HOXD13, since sequenced *Hoxd13* RT-PCR products, using gene specific primers, showed only the mutant transcript is expressed (data not shown). For genes transcriptionally repressed in the HOXA13-expressing cells, *Ngef* and *Casp8ap2*, HOXD13$^{IQN > AAA}$ was unable to repress their expression. However, HOXD13 and HOXA9 repressed these two genes. To test the reproducibility of these results, we verified the differences, by SQ RT-PCR, in an independent preparation of RNA from these same cell lines.

Discussion

In vitro system for identification of HOX-induced downstream gene expression changes

The expression and activity of the evolutionarily conserved transcription factor, HOXA13, is required for the proper development of the limb autopod, umbilical artery, caudal digestive and reproductive tracts (Fromental-Ramain et al., 1996a; Goodman et al., 2000; Innis et al., 2002; Mortlock and Innis, 1997; Mortlock et al., 1996; Stadler et al., 2001; Warot et al., 1997). A disadvantage to using individual *Hox* mutants to identify candidate downstream target genes is their well documented ability to function redundantly (Greer et al., 2000; Rijli and Chambon, 1997; Zakany and Duboule, 1999). Single *Hox* gene mutants phenotypically often look mildly affected or unremarkable compared to wild type mice. Double mutants on the other hand, may lack entire structures, therefore making target gene identification difficult.

To circumvent the problem of functional redundancy, we expressed HOXA13 in mouse embryonic fibroblast cells that do not express paralog group 13 proteins and assessed gene expression changes with high-density gene arrays. A cultured cell line cannot precisely recapitulate the complex dynamics that occur in the developing limb bud. However, the cell line offered the advantage, as recognized by other authors who have used this approach, that the effect of single genes could be explored in relatively homogeneous populations, thereby minimizing the loss of candidate target genes due to heterogeneous tissue effects (Dorsam et al., 2004; Valerius et al., 2002). Combined expression with the HOX cofactor MEIS would be a very interesting experiment to pursue for potential targets regulated through cooperative interactions, and such experiments could be pursued in the future. However, it is important to point out that in the distal limb bud, at least, a combined expression of *Hox* group 13 genes and *Meis* genes does not occur, so perhaps such coexpressed targets might be relevant to another cellular context such as the reproductive tract (Williams et al., 2005).

There were few significant, reproducible expression changes in transinfected cells shortly after infection. This

may be, in part, related to the level of HOX protein expression, which by Western analysis was lower than expected, and certainly lower than in the producer cells. It might be expected based on genetic data that elevated HOX protein dosage may cause more significant changes in downstream gene expression (Zakany et al., 1997). However, we would characterize the expression levels in the HOXA13 stable-expressing cells as near physiologic. Importantly, we expressed only a single HOX protein in these cells. Thus, the contribution of the additional expression of *Hoxd13*, *Hoxd12*, and *Hoxd11*, as observed in the autopod, would likely be increased above the total Hox dose achieved in our cells.

73 probe sets representing 68 separate genes were identified with reproducible expression differences in cells stably-expressing HOXA13 and these differences were verified for several candidates by SQ RT-PCR. For the genes upregulated in the stable HOXA13-expressing cells, expression changes ranged between +30.75-fold to our cut-off of +1.75, and large fold changes were more often observed for genes being expressed at initially low levels in the control cells. Of the genes downregulated in the HOXA13/EGFP-expressing cells, the fold changes were between −5.88 for *Ngef* and −1.75 for *Mox2*. The reproducible changes observed among paralogs, and for some genes with the nonparalog HOXA9, indicate that these cell lines may be useful in the dissection of downstream gene regulatory mechanisms and cis-acting sequences of additional HOX proteins.

Downstream HOX regulated genes

We demonstrated that, for genes upregulated in the HOXA13/EGFP-expressing cells, 11 Gene Ontology (GO) annotations are overrepresented at a significance level of $P < 0.001$. Among the GO terms are cellular components including the “extracellular matrix”, “collagen” and “basement membrane”. Also represented are terms for molecular functions including “extracellular matrix structural constituent” and “extracellular matrix constituent conferring tensile strength”. While not meeting the statistical requirement used in Table 4, another GO term of interest is “extracellular” (P value < 0.005); 48 of the 181 genes in this comparison have this annotation. Together, the data demonstrates that extracellular protein regulation is a major role of HOXA13; the modulation of these extracellular properties is likely to be the primary route by which HOX proteins control cell shape, motility, growth and adhesion.

Among the candidate genes we identified, a few have been found in previous studies to be regulated by HOX proteins and are consistent with a major role for HOX proteins in the regulation of extracellular physiology (Table 5). We identified *Anxa8* and *M32486* as being upregulated by HOXA13. In studies in which the *Hoxa13* homeobox was substituted for that of *Hoxa11*, which drives the expression of a HOXA11 protein with a group 13 homeodomain in the uterus, these two genes were among a set of upregulated genes (Zhao and Potter, 2001). Cell adhesion molecules and ephrin-receptors have emerged as HOX-regulated targets (Stadler et al., 2001; Valerius et al., 2002). HOX proteins of paralog group 1 have been shown to regulate the expression of *EphA2* in the developing hindbrain (Chen and Ruley, 1998; Studer et al., 1998) and HOXA9 regulates the expression of *EphB4* in endothelial cells (Bruhl et al., 2004). The loss of *Hoxa13* expression is associated with the downregulation of *EphA4* and *EphA7* in mutant limb buds and in the umbilical artery (Stadler et al., 2001). Additionally, retroviral misexpression of *Hoxd13* in chicken limb buds was associated with the upregulation of *EphA7* in the autopod, and appeared to require DNA-binding (Caronia et al., 2003). EphrinB1–EphB interactions are required for normal skeletal development, and genetic disruption of this signaling pathway results in polydactyly (Compagni et al., 2003). Here, *EphB3* was upregulated in the HOXA13-expressing cells 1.85-fold, however no change was observed in *EphA4* or *EphA7*. This may be explained by the cellular context used or level of HOXA13 expression. While not meeting our criteria, several genes showed altered expression whose involvement in the extracellular matrix is compelling, including *Ncam* and *Col5a1*, corroborating previous studies demonstrating these as candidate HOX-regulated targets (Jones et al., 1993; Zhao and Potter, 2001).

In the notochord, *Hoxb4* has been shown to upregulate the expression of the pro-apoptotic molecule *Casp8ap2*/*FLASH* (Morgan et al., 2004); in our study, HOXA13 downregulated the transcription of *Casp8ap2*, and this repression required DNA binding (see below). Thus, different paralog groups may regulate the expression of the same genes, but with potentially different outcomes depending on cellular context and/or the specific HOX cofactor(s) involved. The identification of the pro-apoptotic gene *reaper* as a Hox target, in *Drosophila*, suggests that the regulation of cell death is a conserved function of HOX proteins (Lohmann et al., 2002).

Besides the limb bud and caudal female reproductive tract, HOXA13 is expressed in the prostate, umbilical artery,

Table 5
HOXA13-regulated genes also reported in other studies

Candidate target	HOXA13 regulation	Previous result(s)	Reference
M32486	Upregulated	Upregulated	Zhao Y. and Potter S. (2001)
Anxa8	Upregulated	Upregulated	Zhao Y. and Potter S. (2001)
*Col5a1**	Upregulated	Upregulated	Zhao Y. and Potter S. (2001)
Casp8ap2 (FLASH)	Downregulated	Upregulated by HOXB4	Morgan R. et al. (2004)
*Ncam**	Upregulated	Upregulated by HOXB9, B9, and C6	Jones F.S. et al. (1992, 1993)
Integrin a8	No change	Upregulated by HOXA11	Valerius M.T. et al. (2002)

* Meets lower significance criteria: P value <0.05 and a fold change of >1.5.

allantois, migrating myoblasts, and placenta (Mortlock et al., 1996; Podlasek et al., 1999; Stadler et al., 2001; Warot et al., 1997; Yamamoto et al., 1998). Thus, the potential role of some genes identified here as downstream targets may only be confirmed by exploring the relevant tissues. *Fhl1*, the gene with the greatest activation in our experiments, is known to be expressed during early stages of skeletal muscle differentiation (Chu et al., 2000; McGrath et al., 2003). Thus, perhaps this gene is activated by HOXA13 or other posterior HOXA proteins during myoblast migration into the limb (Yamamoto et al., 1998). Similarly, work with *M32486* in the female reproductive tract may be instructive in understanding why HOXA13 so strongly activates its expression in our experimental system and in vivo in *Hoxa11*^{A13HD} mice (Zhao and Potter, 2001). Finally, *Enpp2*/*autotaxin* encodes a bifunctional enzyme with lysophospholipase and phosphodiesterase nucleotide pyrophosphatase activities that is known to strongly regulate tumor and normal cell motility (Hama et al., 2004). Genes involved in the modulation of cell motility have been postulated as Hox realizators (Garcia-Bellido, 1975), thus *Enpp2* is a new candidate target in this category. It is particularly attractive given its downstream position in BMP pathways and perhaps should be examined at later stages of limb morphogenesis or bone maturation in *Hoxa13* mutants. In summary, future studies are needed to define the in vivo contexts wherein these and other candidate downstream targets are regulated by HOXA13 and perhaps other group 13 paralogs.

In vivo regulation of target gene expression

For a selected subset of the candidate downstream genes, the expression pattern was found to be very similar to that of *Hoxa13*, in localizing to the interdigital mesenchyme of the developing autopods. The gene encoding the secreted IGF-signaling antagonist, *Igfbp4*, was shown to require HOXA13 for proper in vivo expression. An absolute loss of expression was not observed in autopodal regions where *Hoxd13* or other posterior *Hoxd* genes are coexpressed, suggesting that *Igfbp4* may be a shared target. At early stages, *Hoxd13* is not expressed in the anterior autopod in the position of developing digit 1 and the first interdigital mesenchyme (ID1; Fig. 4D) unlike that of *Hoxa13* whose expression extends to the anterior-most domain of the autopod (Fig. 4C). The loss in ID1 and the persistent, albeit reduced, expression of *Igfbp4* in ID2–4 of the *Hoxa13* mutant limb buds (compare Figs. 5C,F) may reflect redundant regulation by HOXD13, or other autopod-expressed Hox genes. IGFBP-4 is one of six secreted IGFBPs which is unique from the others in that it functions consistently to inhibit IGF actions (Wetterau et al., 1999). IGFBP4 has been shown to potently block bone cell growth and IGF-mediated cell proliferation (Mohan et al., 1989) and differentiation in various cell types (Zhou et al., 2003). Based on this information, it is plausible that paralog group 13 HOX proteins regulate the expression of IGFBP4 to help direct the sites and/or shape of bone formation within the developing autopod.

Like *Igfbp4*, *Fstl* is expressed in the interdigital mesenchyme of the developing limb buds and encodes a secreted protein whose expression is misregulated in *Hoxa13* mutant limb buds (Fig. 6). FSTL is one of many BMP-signaling antagonists, such as follistatin, chordin, and noggin, that function through interaction with signaling ligands preventing interaction with their cellular receptors (Canalis et al., 2003). BMP-signaling induces mesenchymal cells to differentiate into cells of the osteoblastic lineage (Gitelman et al., 1995; Yamaguchi et al., 1996). The overexpression of BMP-2 and BMP-4 in the developing limbs results in an increase in cartilage cell number and in matrix cartilage (Duprez et al., 1996). During limb development, BMP-signaling has been demonstrated to promote interdigital apoptosis and inhibition results in syndactyly (Yokouchi et al., 1996; Zou and Niswander, 1996). Therefore, the regulation of *Fstl* by HOXA13 may influence mesenchymal cell differentiation and the onset of cell death. Whether or not this plays a role in the interdigital syndactyly observed in ID1 in *Hoxa13*$^{-/-}$ mutants is unknown.

How many downstream genes do HOX proteins regulate?

The ability of HOX proteins to regulate morphogenesis has long been hypothesized to operate through the regulation of many genes, known as realizators, whose encoded proteins directly function in the processes such as cell shape, division, survival, apoptosis, motility, adhesion, and differentiation (Garcia-Bellido, 1975). This hypothesis has largely been proven correct, and recent work has demonstrated that HOX proteins can also regulate the expression of other transcription factors as well as signaling molecules (Weatherbee et al., 1998). An important question in understanding HOX function is how many genes are subject to HOX regulation? Several studies, in *Drosophila*, have shown that HOX proteins are bound to many sites within the genome (Biggin and McGinnis, 1997; Walter et al., 1994), and that greater than 25% of expressed genes are directly or indirectly regulated by HOX proteins (Liang and Biggin, 1998). In contrast, in our study, we estimate that fewer than 1% of the genes (68/~9000) on the chip are regulated by HOXA13 expression. The low percentage of targets observed here is consistent with the findings of other studies that explored a large number of genes as potential HOX targets (Hedlund et al., 2004; Valerius et al., 2002; Zhao and Potter, 2001). However, perhaps the cellular context, availability of chromatin, or cofactor expression limited the number of observed expression changes in our experiments. It is also possible that higher levels of group 13 protein expression could cause greater expression changes and may mimic the expression of multiple paralogs in the same cell.

Mode of downstream target gene regulation

A shared feature of all HOX proteins is the presence of a 60 amino acid homeodomain, which is well known for its ability to bind DNA. The regulation of transcriptional targets by HOX proteins has been shown to occur through DNA target-site recognition and binding by this protein domain with (Mann and Affolter, 1998; Mann and Morata, 2000) or without cofactors (Galant et al., 2002). There is a significant body of literature, primarily from *Drosophila* studies, demonstrating in vivo function by these means (Gebelein et al., 2002; Kobayashi et al., 2003). To our surprise, HOXD13$^{IQN > AAA}$, a protein incapable of binding to DNA as a monomer, is fully capable of upregulating the expression of 5 tested genes (*Blnk*, *Enpp2*, *Fabp4*, *Fhl1*, and *Ifit1*). Conversely, HOXD13 and HOXA9 were shown to downregulate *Casp8ap2* and *Ngef*, however HOXD13$^{IQN > AAA}$ could not. Thus, with this limited number of downstream genes, paralog group 13 HOX proteins can act as transcriptional activators even though incapable of binding DNA as a monomer. Repression, in our data, requires the ability to bind DNA and can be accomplished on common genes by a non-paralogous (HOXA9) protein. Similar findings were observed for HOXC8 repression on *Osteopontin* and *Osteoprotegrin* promoter activity (Shi et al., 1999; Wan et al., 2001). Mutation of the HOXC8 binding-site was shown to abolish HOX-mediated repression.

Homeodomain proteins have been shown to retain function in the absence of DNA-binding. Mutants of the *Drosophila* homeodomain protein Ftz, with either altered DNA-binding specificity or inability to bind DNA, retain substantial wild type function, suggesting that some Ftz targets are regulated through protein–protein interactions (Ananthan et al., 1993; Copeland et al., 1996; Fitzpatrick et al., 1992; Hyduk and Percival-Smith, 1996; Schier and Gehring, 1993). Similar findings were demonstrated for the yeast α2 homeodomain repressor protein, where the direct regulation of targets by mutant monomeric α2 as well as α2/MCM1 heterodimer was impaired. However, identical α2 mutants still retained the ability to cooperatively bind DNA with a1 to effectively repress haploid specific genes in vivo (Vershon et al., 1995). DNA binding-independent functions of HOX proteins have also been observed in vertebrates. The antagonistic effect of HOXD8 on HOXD9 autoregulation, through the HCR element, is DNA-binding independent and likely mediated through protein–protein interactions (Zappavigna et al., 1994). A DNA-binding impaired HOXD12 can effectively convert the GLI3 repressor into a transcriptional activator (Chen et al., 2004). Additionally, HOXA13 with the homeodomain deleted still appears capable of acting as a strong transcriptional activator of the *Bmp-4* promoter (Suzuki et al., 2003). Furthermore, the homeodomains of HOX proteins from multiple paralog groups, including group 13, have been shown to interact with CBP (Shen et al., 2001). Interestingly, interaction with CBP not only inhibited DNA-binding of HOX proteins, but also inhibited the histone acetyltransferase activity of CBP. The lysine at position 55 of the third helix of the HOXB7 homeodomain was necessary for this in vivo function. Thus, it would be interesting to test whether lysine 55 in the group 13 HOX proteins is necessary for the transcriptional effects we measured.

In summary, while DNA-binding independent functions have been an observed mechanism of HOX function, the frequent observation in our studies of this activity in downstream gene activation was unexpected. Thus, we wish to amplify the proposal of Shen et al., 2001, that HOX protein functions are not limited to DNA bound activities, by suggesting that the prevalence of HOX proteins regulating gene expression as the non DNA-binding partner or in solution off of DNA with a cofactor could be much greater than generally assumed.

Acknowledgments

We thank Frank Urban for his technical assistance with retroviral methods, Shannon Davis and Sally Camper for supplying templates for *Fstl* and *EphB3* antisense probes, and technicians of the University of Michigan Flow Cytometry Core for cell separations. T.M. Williams and M.E. Williams were supported in part by a NIH Genetics Training Grant Fellowship (T32 GM07544). This work was supported by grants from the NIH (RO1 HD37486) and the University of Michigan Rheumatic Diseases Core Center.

References

Ananthan, J., Baler, R., Morrissey, D., Zuo, J., Lan, Y., Weir, M., Voellmy, R., 1993. Synergistic activation of transcription is mediated by the N-terminal domain of *Drosophila fushi tarazu* homeoprotein and can occur without DNA binding by the protein. Mol. Cell. Biol. 13, 1599–1609.

Bachner, D., Ahrens, M., Schroder, D., Hoffmann, A., Lauber, J., Betat, N., Steinert, P., Flohe, L., Gross, G., 1998. Bmp-2 downstream targets in mesenchymal development identified by subtractive cloning from recombinant mesenchymal progenitors (C3H10T1/2). Dev. Dyn. 213, 398–411.

Bachner, D., Ahrens, M., Betat, N., Schroder, D., Gross, G., 1999. Developmental expression analysis of murine autotaxin (ATX). Mech. Dev. 84, 121–125.

Baigent, S.M., Lowry, P.J., 2000. mRNA expression profiles for corticotrophin-releasing factor (CRF), urocortin, CRF receptors and CRF-binding protein in peripheral rat tissues. J. Mol. Endocrinol. 25, 43–52.

Beer, D.G., Kardia, S.L., Huang, C.C., Giordano, T.J., Levin, A.M., Misek, D.E., Lin, L., Chen, G., Gharib, T.G., Thomas, D.G., Lizyness, M.L., Kuick, R., Hayasaka, S., Taylor, J.M., Iannettoni, M.D., Orringer, M.B., Hanash, S., 2002. Gene-expression profiles predict survival of patients with lung adenocarcinoma. Nat. Med. 8, 816–824.

Biggin, M.D., McGinnis, W., 1997. Regulation of segmentation and segmental identity by *Drosophila* homeoproteins: the role of DNA binding in functional activity and specificity. Development 124, 4425–4433.

Bober, E., Franz, T., Arnold, H.H., Gruss, P., Tremblay, P., 1994. Pax-3 is

required for the development of limb muscles: a possible role for the migration of dermomyotomal muscle progenitor cells. Development 120, 603–612.

Boudreau, N.J., Varner, J.A., 2004. The homeobox transcription factor Hox D3 promotes integrin alpha5beta1 expression and function during angiogenesis. J. Biol. Chem. 279, 4862–4868.

Bromleigh, V.C., Freedman, L.P., 2000. p21 Is a transcriptional target of HOXA10 in differentiating myelomonocytic cells. Genes Dev. 14, 2581–2586.

Bruhl, T., Urbich, C., Aicher, D., Acker-Palmer, A., Zeiher, A.M., Dimmeler, S., 2004. Homeobox A9 transcriptionally regulates the EphB4 receptor to modulate endothelial cell migration and tube formation. Circ. Res. 94, 743–751.

Canalis, E., Economides, A.N., Gazzerro, E., 2003. Bone morphogenetic proteins, their antagonists, and the skeleton. Endocr. Rev. 24, 218–235.

Caronia, G., Goodman, F.R., McKeown, C.M., Scambler, P.J., Zappavigna, V., 2003. An I47L substitution in the HOXD13 homeodomain causes a novel human limb malformation by producing a selective loss of function. Development 130, 1701–1712.

Chen, J., Ruley, H.E., 1998. An enhancer element in the EphA2 (Eck) gene sufficient for rhombomere-specific expression is activated by HOXA1 and HOXB1 homeobox proteins. J. Biol. Chem. 273, 24670–24675.

Chen, Y., Knezevic, V., Ervin, V., Hutson, R., Ward, Y., Mackem, S., 2004. Direct interaction with Hoxd proteins reverses Gli3-repressor function to promote digit formation downstream of Shh. Development 131, 2339–2347.

Chu, P.H., Ruiz-Lozano, P., Zhou, Q., Cai, C., Chen, J., 2000. Expression patterns of FHL/SLIM family members suggest important functional roles in skeletal muscle and cardiovascular system. Mech. Dev. 95, 259–265.

Compagni, A., Logan, M., Klein, R., Adams, R.H., 2003. Control of skeletal patterning by ephrinB1-EphB interactions. Dev. Cell 5, 217–230.

Copeland, J.W., Nasiadka, A., Dietrich, B.H., Krause, H.M., 1996. Patterning of the *Drosophila* embryo by a homeodomain-deleted Ftz polypeptide. Nature 379, 162–165.

Creighton, C., Kuick, R., Misek, D.E., Rickman, D.S., Brichory, F.M., Rouillard, J.M., Omenn, G.S., Hanash, S., 2003. Profiling of pathway-specific changes in gene expression following growth of human cancer cell lines transplanted into mice. Genome Biol. 4, R46.

Dorsam, S.T., Ferrell, C.M., Dorsam, G.P., Derynck, M.K., Vijapurkar, U., Khodabakhsh, D., Pau, B., Bernstein, H., Haqq, C.M., Largman, C., Lawrence, H.J., 2004. The transcriptome of the leukemogenic homeoprotein HOXA9 in human hematopoietic cells. Blood 103, 1676–1684.

Duboule, D., Morata, G., 1994. Colinearity and functional hierarchy among genes of the homeotic complexes. Trends Genet. 10, 358–364.

Duprez, D., Bell, E.J., Richardson, M.K., Archer, C.W., Wolpert, L., Brickell, P.M., Francis-West, P.H., 1996. Overexpression of BMP-2 and BMP-4 alters the size and shape of developing skeletal elements in the chick limb. Mech. Dev. 57, 145–157.

Edelman, G.M., Jones, F.S., 1995. Developmental control of N-CAM expression by Hox and Pax gene products. Philos. Trans. R. Soc. Lond., Ser. B Biol. Sci. 349, 305–312.

Favier, B., Rijli, F.M., Fromental-Ramain, C., Fraulob, V., Chambon, P., Dolle, P., 1996. Functional cooperation between the non-paralogous genes Hoxa-10 and Hoxd-11 in the developing forelimb and axial skeleton. Development 122, 449–460.

Ferretti, E., Marshall, H., Popperl, H., Maconochie, M., Krumlauf, R., Blasi, F., 2000. Segmental expression of Hoxb2 in r4 requires two separate sites that integrate cooperative interactions between Prep1, Pbx and Hox proteins. Development 127, 155–166.

Fitzpatrick, V.D., Percival-Smith, A., Ingles, C.J., Krause, H.M., 1992. Homeodomain-independent activity of the fushi tarazu polypeptide in *Drosophila* embryos. Nature 356, 610–612.

Fromental-Ramain, C., Warot, X., Lakkaraju, S., Favier, B., Haack, H., Birling, C., Dierich, A., Doll e, P., Chambon, P., 1996a. Specific and redundant functions of the paralogous Hoxa-9 and Hoxd-9 genes in forelimb and axial skeleton patterning. Development 122, 461–472.

Fromental-Ramain, C., Warot, X., Messadecq, N., LeMeur, M., Dolle, P., Chambon, P., 1996b. Hoxa-13 and Hoxd-13 play a crucial role in the patterning of the limb autopod. Development 122, 2997–3011.

Galant, R., Walsh, C.M., Carroll, S.B., 2002. Hox repression of a target gene: extradenticle-independent, additive action through multiple monomer binding sites. Development 129, 3115–3126.

Garcia-Bellido, A., 1975. Genetic control of wing disc development in *Drosophila*. Ciba Found. Symp. 0, 161–182.

Gebelein, B., Culi, J., Ryoo, H.D., Zhang, W., Mann, R.S., 2002. Specificity of Distalless repression and limb primordia development by abdominal Hox proteins. Dev. Cell 3, 487–498.

Gehring, W.J., Affolter, M., Burglin, T., 1994a. Homeodomain proteins. Annu. Rev. Biochem. 63, 487–526.

Gehring, W.J., Qian, Y.Q., Billeter, M., Furukubo-Tokunaga, K., Schier, A.F., Resendez-Perez, D., Affolter, M., Otting, G., Wuthrich, K., 1994b. Homeodomain-DNA recognition. Cell 78, 211–223.

Gitelman, S.E., Kirk, M., Ye, J.Q., Filvaroff, E.H., Kahn, A.J., Derynck, R., 1995. Vgr-1/BMP-6 induces osteoblastic differentiation of pluripotential mesenchymal cells. Cell Growth Differ. 6, 827–836.

Goff, D.J., Tabin, C.J., 1997. Analysis of Hoxd-13 and Hoxd-11 misexpression in chick limb buds reveals that Hox genes affect both bone condensation and growth. Development 124, 627–636.

Goodman, F.R., Bacchelli, C., Brady, A.F., Brueton, L.A., Fryns, J.P., Mortlock, D.P., Innis, J.W., Holmes, L.B., Donnenfeld, A.E., Feingold, M., Beemer, F.A., Hennekam, R.C., Scambler, P.J., 2000. Novel HOXA13 mutations and the phenotypic spectrum of hand–foot–genital syndrome. Am. J. Hum. Genet. 67, 197–202.

Goomer, R.S., Holst, B.D., Wood, I.C., Jones, F.S., Edelman, G.M., 1994. Regulation in vitro of an L-CAM enhancer by homeobox genes HoxD9 and HNF-1. Proc. Natl. Acad. Sci. U. S. A. 91, 7985–7989.

Greer, J.M., Puetz, J., Thomas, K.R., Capecchi, M.R., 2000. Maintenance of functional equivalence during paralogous Hox gene evolution. Nature 403, 661–665.

Hama, K., Aoki, J., Fukaya, M., Kishi, Y., Sakai, T., Suzuki, R., Ohta, H., Yamori, T., Watanabe, M., Chun, J., Arai, H., 2004. Lysophosphatidic acid and autotaxin stimulate cell motility of neoplastic and non-neoplastic cells through LPA1. J. Biol. Chem. 279, 17634–17639.

Hedlund, E., Karsten, S.L., Kudo, L., Geschwind, D.H., Carpenter, E.M., 2004. Identification of a Hoxd10-regulated transcriptional network and combinatorial interactions with Hoxa10 during spinal cord development. J. Neurosci. Res. 75, 307–319.

Hyduk, D., Percival-Smith, A., 1996. Genetic characterization of the homeodomain-independent activity of the *Drosophila* fushi tarazu gene product. Genetics 142, 481–492.

Innis, J.W., Goodman, F.R., Bacchelli, C., Williams, T.M., Mortlock, D.P., Sateesh, P., Scambler, P.J., McKinnon, W., Guttmacher, A.E., 2002. A HOXA13 allele with a missense mutation in the homeobox and a dinucleotide deletion in the promoter underlies Guttmacher syndrome. Hum. Mutat. 19, 573–574.

Jacobs, Y., Schnabel, C.A., Cleary, M.L., 1999. Trimeric association of Hox and TALE homeodomain proteins mediates Hoxb2 hindbrain enhancer activity. Mol. Cell. Biol. 19, 5134–5142.

Jones, F.S., Prediger, E.A., Bittner, D.A., De Robertis, E.M., Edelman, G.M., 1992. Cell adhesion molecules as targets for Hox genes: neural cell adhesion molecule promoter activity is modulated by cotransfection with Hox-2.5 and -2.4. Proc. Natl. Acad. Sci. U. S. A. 89, 2086–2090.

Jones, F.S., Holst, B.D., Minowa, O., De Robertis, E.M., Edelman, G.M., 1993. Binding and transcriptional activation of the promoter for the neural cell adhesion molecule by HoxC6 (Hox-3.3). Proc. Natl. Acad. Sci. U. S. A. 90, 6557–6561.

Kondo, T., Zakany, J., Duboule, D., 1998. Control of colinearity in AbdB genes of the mouse HoxD complex. Mol. Cell 1, 289–300.

Krumlauf, R., 1994. Hox genes in vertebrate development. Cell 78, 191–201.

LaRonde-LeBlanc, N.A., Wolberger, C., 2003. Structure of HoxA9 and

Pbx1 bound to DNA: Hox hexapeptide and DNA recognition anterior to posterior. Genes Dev. 17, 2060–2072.
Laughon, A., 1991. DNA binding specificity of homeodomains. Biochemistry 30, 11357–11367.
Lee, K.K., Tang, M.K., Yew, D.T., Chow, P.H., Yee, S.P., Schneider, C., Brancolini, C., 1999. gas2 is a multifunctional gene involved in the regulation of apoptosis and chondrogenesis in the developing mouse limb. Dev. Biol. 207, 14–25.
Liang, Z., Biggin, M.D., 1998. Eve and ftz regulate a wide array of genes in blastoderm embryos: the selector homeoproteins directly or indirectly regulate most genes in *Drosophila*. Development 125, 4471–4482.
Lohmann, I., McGinnis, N., Bodmer, M., McGinnis, W., 2002. The *Drosophila* Hox gene deformed sculpts head morphology via direct regulation of the apoptosis activator reaper. Cell 110, 457–466.
Mann, R.S., Affolter, M., 1998. Hox proteins meet more partners. Curr. Opin. Genet. Dev. 8, 423–429.
Mann, R.S., Morata, G., 2000. The developmental and molecular biology of genes that subdivide the body of *Drosophila*. Annu. Rev. Cell Dev. Biol. 16, 243–271.
Markowitz, D., Hesdorffer, C., Ward, M., Goff, S., Bank, A., 1990. Retroviral gene transfer using safe and efficient packaging cell lines. Ann. N. Y. Acad. Sci. 612, 407–414.
McGinnis, W., Krumlauf, R., 1992. Homeobox genes and axial patterning. Cell 68, 283–302.
McGrath, M.J., Mitchell, C.A., Coghill, I.D., Robinson, P.A., Brown, S., 2003. Skeletal muscle LIM protein 1 (SLIM1/FHL1) induces alpha 5 beta 1-integrin-dependent myocyte elongation. Am. J. Physiol.: Cell Physiol. 285, C1513–C1526.
Mohan, S., Bautista, C.M., Wergedal, J., Baylink, D.J., 1989. Isolation of an inhibitory insulin-like growth factor (IGF) binding protein from bone cell-conditioned medium: a potential local regulator of IGF action. Proc. Natl. Acad. Sci. U. S. A. 86, 8338–8342.
Morgan, R., Nalliah, A., Morsi El-Kadi, A.S., 2004. FLASH, a component of the FAS-CAPSASE8 apoptotic pathway, is directly regulated by Hoxb4 in the notochord. Dev. Biol. 265, 105–112.
Mortlock, D.P., Innis, J.W., 1997. Mutation of HOXA13 in hand–foot–genital syndrome. Nat. Genet. 15, 179–180.
Mortlock, D.P., Post, L.C., Innis, J.W., 1996. The molecular basis of hypodactyly (Hd): a deletion in Hoxa 13 leads to arrest of digital arch formation. Nat. Genet. 13, 284–289.
Podlasek, C.A., Clemens, J.Q., Bushman, W., 1999. Hoxa-13 gene mutation results in abnormal seminal vesicle and prostate development. J. Urol. 161, 1655–1661.
Post, L.C., Innis, J.W., 1999a. Altered Hox expression and increased cell death distinguish Hypodactyly from Hoxa13 null mice. Int. J. Dev. Biol. 43, 287–294.
Post, L.C., Innis, J.W., 1999b. Infertility in adult hypodactyly mice is associated with hypoplasia of distal reproductive structures. Biol. Reprod. 61, 1402–1408.
Post, L.C., Margulies, E.H., Kuo, A., Innis, J.W., 2000. Severe limb defects in Hypodactyly mice result from the expression of a novel, mutant HOXA13 protein. Dev. Biol. 217, 290–300.
Rijli, F.M., Chambon, P., 1997. Genetic interactions of Hox genes in limb development: learning from compound mutants. Curr. Opin. Genet. Dev. 7, 481–487.
Rosen, V., Nove, J., Song, J.J., Thies, R.S., Cox, K., Wozney, J.M., 1994. Responsiveness of clonal limb bud cell lines to bone morphogenetic protein 2 reveals a sequential relationship between cartilage and bone cell phenotypes. J. Bone Miner. Res. 9, 1759–1768.
Ruddle, F.H., Bartels, J.L., Bentley, K.L., Kappen, C., Murtha, M.T., Pendleton, J.W., 1994. Evolution of Hox genes. Annu. Rev. Genet. 28, 423–442.
Schier, A.F., Gehring, W.J., 1993. Functional specificity of the homeodomain protein fushi tarazu: the role of DNA-binding specificity in vivo. Proc. Natl. Acad. Sci. U. S. A. 90, 1450–1454.
Schwartz, D.R., Kardia, S.L., Shedden, K.A., Kuick, R., Michailidis, G., Taylor, J.M., Misek, D.E., Wu, R., Zhai, Y., Darrah, D.M., Reed, H., Ellenson, L.H., Giordano, T.J., Fearon, E.R., Hanash, S.M., Cho, K.R., 2002. Gene expression in ovarian cancer reflects both morphology and biological behavior, distinguishing clear cell from other poor-prognosis ovarian carcinomas. Cancer Res. 62, 4722–4729.
Shen, W.F., Krishnan, K., Lawrence, H.J., Largman, C., 2001. The HOX homeodomain proteins block CBP histone acetyltransferase activity. Mol. Cell. Biol. 21, 7509–7522.
Shi, X., Yang, X., Chen, D., Chang, Z., Cao, X., 1999. Smad1 interacts with homeobox DNA-binding proteins in bone morphogenetic protein signaling. J. Biol. Chem. 274, 13711–13717.
Stadler, H.S., Higgins, K.M., Capecchi, M.R., 2001. Loss of Eph-receptor expression correlates with loss of cell adhesion and chondrogenic capacity in Hoxa13 mutant limbs. Development 128, 4177–4188.
Studer, M., Gavalas, A., Marshall, H., Ariza-McNaughton, L., Rijli, F.M., Chambon, P., Krumlauf, R., 1998. Genetic interactions between Hoxa1 and Hoxb1 reveal new roles in regulation of early hindbrain patterning. Development 125, 1025–1036.
Suzuki, M., Kuroiwa, A., 2002. Transition of Hox expression during limb cartilage development. Mech. Dev. 118, 241–245.
Suzuki, M., Ueno, N., Kuroiwa, A., 2003. Hox proteins functionally cooperate with the GC box-binding protein system through distinct domains. J. Biol. Chem. 278, 30148–30156.
Taylor, H.S., Vanden Heuvel, G.B., Igarashi, P., 1997. A conserved Hox axis in the mouse and human female reproductive system: late establishment and persistent adult expression of the Hoxa cluster genes. Biol. Reprod. 57, 1338–1345.
Tusher, V.G., Tibshirani, R., Chu, G., 2001. Significance analysis of microarrays applied to the ionizing radiation response. Proc. Natl. Acad. Sci. U. S. A. 98, 5116–5121.
Valerius, M.T., Patterson, L.T., Feng, Y., Potter, S.S., 2002. Hoxa 11 is upstream of Integrin alpha8 expression in the developing kidney. Proc. Natl. Acad. Sci. U. S. A. 99, 8090–8095.
Vershon, A.K., Jin, Y., Johnson, A.D., 1995. A homeo domain protein lacking specific side chains of helix 3 can still bind DNA and direct transcriptional repression. Genes Dev. 9, 182–192.
Walter, J., Dever, C.A., Biggin, M.D., 1994. Two homeo domain proteins bind with similar specificity to a wide range of DNA sites in *Drosophila* embryos. Genes Dev. 8, 1678–1692.
Wan, M., Shi, X., Feng, X., Cao, X., 2001. Transcriptional mechanisms of bone morphogenetic protein-induced osteoprotegrin gene expression. J. Biol. Chem. 276, 10119–10125.
Wanek, N., Muneoka, K., Holler-Dinsmore, G., Burton, R., Bryant, S.V., 1989. A staging system for mouse limb development. J. Exp. Zool. 249, 41–49.
Warot, X., Fromental-Ramain, C., Fraulob, V., Chambon, P., Dolle, P., 1997. Gene dosage-dependent effects of the Hoxa-13 and Hoxd-13 mutations on morphogenesis of the terminal parts of the digestive and urogenital tracts. Development 124, 4781–4791.
Weatherbee, S.D., Halder, G., Kim, J., Hudson, A., Carroll, S., 1998. Ultrabithorax regulates genes at several levels of the wing-patterning hierarchy to shape the development of the *Drosophila* haltere. Genes Dev. 12, 1474–1482.
Wellik, D.M., Capecchi, M.R., 2003. Hox10 and Hox11 genes are required to globally pattern the mammalian skeleton. Science 301, 363–367.
Wetterau, L.A., Moore, M.G., Lee, K.W., Shim, M.L., Cohen, P., 1999. Novel aspects of the insulin-like growth factor binding proteins. Mol. Genet. Metab. 68, 161–181.
Williams, T.M., Williams, M.E., Innis, J.W., 2005. Range of HOX/TALE Superclass Associations and Protein Domain Requirements for HOX-A13:MEIS Interaction. Dev. Biol. 277, 457–471
Yamaguchi, A., Ishizuya, T., Kintou, N., Wada, Y., Katagiri, T., Wozney, J.M., Rosen, V., Yoshiki, S., 1996. Effects of BMP-2, BMP-4, and BMP-6 on osteoblastic differentiation of bone marrow-derived stromal cell lines, ST2 and MC3T3-G2/PA6. Biochem. Biophys. Res. Commun. 220, 366–371.

Yamamoto, M., Gotoh, Y., Tamura, K., Tanaka, M., Kawakami, A., Ide, H., Kuroiwa, A., 1998. Coordinated expression of Hoxa-11 and Hoxa-13 during limb muscle patterning. Development 125, 1325–1335.

Yang, J., Friedman, M.S., Bian, H., Crofford, L.J., Roessler, B., McDonagh, K.T., 2002. Highly efficient genetic transduction of primary human synoviocytes with concentrated retroviral supernatant. Arthritis Res. 4, 215–219.

Yokouchi, Y., Sakiyama, J., Kameda, T., Iba, H., Suzuki, A., Ueno, N., Kuroiwa, A., 1996. BMP-2/-4 mediate programmed cell death in chicken limb buds. Development 122, 3725–3734.

Zakany, J., Duboule, D., 1996. Synpolydactyly in mice with a targeted deficiency in the HoxD complex. Nature 384, 69–71.

Zakany, J., Duboule, D., 1999. Hox genes in digit development and evolution. Cell Tissue Res. 296, 19–25.

Zakany, J., Fromental-Ramain, C., Warot, X., Duboule, D., 1997. Regulation of number and size of digits by posterior Hox genes: a dose-dependent mechanism with potential evolutionary implications. Proc. Natl. Acad. Sci. U. S. A. 94, 13695–13700.

Zappavigna, V., Sartori, D., Mavilio, F., 1994. Specificity of HOX protein function depends on DNA–protein and protein–protein interactions, both mediated by the homeo domain. Genes Dev. 8, 732–744.

Zhao, Y., Potter, S.S., 2001. Functional specificity of the Hoxa13 homeobox. Development 128, 3197–3207.

Zhao, Y., Potter, S.S., 2002. Functional comparison of the Hoxa 4, Hoxa 10, and Hoxa 11 homeoboxes. Dev. Biol. 244, 21–36.

Zhou, R., Diehl, D., Hoeflich, A., Lahm, H., Wolf, E., 2003. IGF-binding protein-4: biochemical characteristics and functional consequences. J. Endocrinol. 178, 177–193.

Zou, H., Niswander, L., 1996. Requirement for BMP signaling in interdigital apoptosis and scale formation. Science 272, 738–741.